The Histology of Ossification in the Caudal Fin of Larval Zebrafish, *Danio rerio*

By Nicole C. Daley

A thesis submitted to

Saint Mary's University, Halifax, Nova Scotia

In Partial Fulfillment of the Requirements for the Degree of Bachelor of Science with Honours

April 14, 2023, Halifax, Nova Scotia

Approved: _____

Dr. Tamara Franz-Odendaal

Approved: _____

Dr. Michelle Patriquin

Date: _____

Abstract – Nicole Daley - The Histology of Ossification in the Caudal Fin of Larval Zebrafish, *Danio rerio* – May 1, 2023

Endochondral ossification is a bone developing process in which a cartilaginous template gets replaced by bone. Zebrafish, *Danio rerio,* are teleost fish that undergo this process throughout their skeletons. This thesis is focussed on their tail bones, specifically within the hypurals and parhypural of the caudal fin. The morphological changes in the cells of the hypurals and parhypural during ossification have not been recorded so the aim of this study is to investigate these changes taking a histological approach. To determine the morphological cellular changes Hall Brunt's Quadruple staining was used to stain the bone and cartilage within zebrafish sized 4 to 9 mm standard length. Changes within the chondrocytes were measured and descriptions of the amount of ossification were made. It was found that all five hypurals and the parhypural begin ossifying around 5.0 mm SL, while the chondrocytes underwent hypertrophy by 7.0 mm SL there was a lower percentage of hypertrophied chondrocytes in 8.0 – 9.0 mm SL specimens for hypurals 2 and 3. Hypural 2 and 3 were the elements primarily focused on, that had an increase in total hypural length (μm). These results suggest that the hypurals share features of both endochondral and perichondral ossification. Further studies are needed to further understand ossification within the zebrafish caudal fin.

Table of Contents

Table of Figures

Table of tables

1 Introduction

1.1 Cartilage

Cartilage is a connective tissue that provides structure and rigidity to the skeleton. It is composed primarily of an extracellular matrix produced by chondrocytes, which is what provides the rigidity (Stockwell, 1978). Along with the matrix, chondrocytes also secrete collagen type II (Stockwell, 1978). Chondrocytes arise from the differentiation of condensations, which are densely packed mesenchymal cells, that are formed in early embryonic stages (Felber et al., 2010). Cartilage can be permanent or temporary, with temporary cartilage undergoing ossification. The matrix created by the chondrocytes provides a cartilaginous template for bone formation in both perichondral and endochondral ossification. This process occurs during the development of the organism as the skeleton grows.

1.2 Bone

Bone is a living tissue that is one of the components of the skeleton of an organism. Bone is composed of: hydroxyapatite, which consists of calcium and phosphate; a bone matrix, which is primarily composed of collagen type I and other proteins; and water (Boskey, 2013). Bone is composed of several different cell types including: osteocytes, osteoblasts, and osteoclasts. Osteoblasts, bone-forming cells, are derived from mesenchymal cells, which are undifferentiated embryonic cells (Ding et al., 2011; Kobayashi-Sun et al., 2020). Osteoblasts are responsible for secreting the bone matrix including collagen type I, and become embedded in the matrix as osteocytes. During this process, osteoblasts undergo a physical change into osteocytes, losing volume in their cell bodies and forming cell processes (Franz-Odendaal et al., 2006; Kobayashi-Sun et al., 2020). Osteoclasts are another bone cell type, which differentiate from hematopoietic stem cells, responsible for resorbing the bone matrix, causing it to degrade (Kobayashi-Sun et al., 2020; Odgren et al., 2016). The balance between the deposition of bone from osteoblasts and resorption by osteoclasts helps to maintain bone homeostasis.

1.3 Osteogenesis and the role of cartilage

Osteogenesis is the formation of bone and bone cells within organisms. There are several different types of ossification, including: intramembranous ossification, perichondral ossification and endochondral ossification. The general process of skeletal formation -includes the differentiation of mesenchymal cells into condensations. From the condensations either chondrocytes or osteoblasts will differentiate (Ding et al., 2011; Franz-Odendaal et al., 2006; Grandel & Schulte-Merker, 1998; Weigele & Franz-Odendaal, 2016). Intramembranous ossification occurs after mesenchymal cells form condensations of osteoblasts. These cells differentiate into osteocytes and deposit bone matrix directly without the involvement of a cartilage phase (Franz-Odendaal et al., 2006; Grandel & Schulte-Merker, 1998; Weigele & Franz-Odendaal, 2016). Perichondral ossification and endochondral ossification both require a cartilaginous template that will ultimately be replaced by bone (Felber et al., 2010; Weigele & Franz-Odendaal, 2016). The chondrocytes that make up the cartilaginous template undergo several changes before bone begins to form. The chondrocytes will undergo hypertrophy, increasing in size, then undergo regulated cell death before bone will begin to form (Weigele & Franz-Odendaal, 2016). The hypertrophied chondrocytes forms two distinct zones, one of hypertrophied chondrocytes, and a zone of flattened chondrocytes (cells that have not yet undergone hypertrophy). For perichondral ossification, bone matrix is secreted from within the perichondrium (a connective tissue sheath that surrounds cartilage), following the differentiation of osteoblasts in this layer (Felber et al., 2010). That is, ossification occurs from the outside of the cartilage template inwards. In endochondral ossification the cartilaginous template gets replaced by bone from within the cartilage template. Endochondral ossification is the most common form of ossification in mammals and typically found in long bones (Felber et al., 2010;

Heubel et al., 2021; Mackie et al., 2008). The two types of ossification result in different types of bones, with perichondral ossification developing cortical bone and endochondral ossification developing trabecular bone(Cervantes-Diaz et al., 2017).

There are several cellular changes that occur throughout the ossification process. These changes begin for endochondral and perichondral ossification (cartilage being replaced by bone) with changes to the chondrocytes. Chondrocytes rapidly increase in number, and undergo hypertrophy before going through apoptosis during the initial stages of endochondral ossification (Mackie et al., 2008). After this, osteoblasts and osteoclasts arrive in the extracellular matrix of the cartilage template in a zone of degradation, which is where the cartilage begins to degrade (Mackie et al., 2008; Weigele & Franz-Odendaal, 2016). This results in the cartilage becoming replaced by bone, and ultimately completing ossification. There are two types of endochondral ossification found within adult zebrafish. Type I is endochondral ossification as described above, while type II does not have the zone of degradation, but has active chondroclasts, cartilage resorbing cells, instead (these cells can also be found in Type I) (Knowles et al., 2012; Weigele & Franz-Odendaal, 2016). This second type of ossification produces tubular bones that are filled only with adipose (fat) tissue, rather than a trabeculae network that is found in type I endochondral ossification (Weigele & Franz-Odendaal, 2016).

1.4 Zebrafish

Zebrafish, *Danio rerio*, have been used as model systems to study many different biological mechanisms (Briggs, 2002; Busse et al., 2020; Gemberling et al., 2013; Mione & Trede, 2010). Zebrafish are small aquatic fish with their maximum size ranging between 3 and 4 cm in adults (Tonelli et al., 2020). This small size allows the entire larval zebrafish to be wax embedded for histological sectioning, rather than requiring dissections prior embedding. Another

aspect of zebrafish that makes them a good model organism is their rapid growth. Within 90 days post-fertilization (dpf), a zebrafish will have grown to adulthood (Copper et al., 2018; Dietrich et al., 2021). This short growth time provides researchers the ability to investigate every stage of zebrafish within 3 months. Larval zebrafish develop quickly, so using them as a model organism allows researchers to study development easily, especially in bones.

Ossification begins to occur in all elements of the axial skeleton between 30-44 dpf, due to this quick development (Bird & Mabee, 2003; Copper et al., 2018). The axial skeleton of fish includes the vertebral column and the unpaired fins (dorsal, anal and caudal fins) (entire skeleton shown in Figure 1) (Bird & Mabee, 2003). Zebrafish have similar skeletal cell types to those of mammals (Tonelli et al., 2020). The skeleton also undergoes similar methods of ossification as mammals and the same bone and cartilage cell types are found in all vertebrates, meaning that studying these processes in zebrafish provides knowledge about them in mammals as well (Weigele & Franz-Odendaal, 2016). This model organism has therefore been used to understand human biology, especially in regard to the skeleton (e.g. Tonelli et al., 2020). Furthermore, the zebrafish is able to provide information on skeletal diseases as well as development of bones in humans (Tonelli et al., 2020).

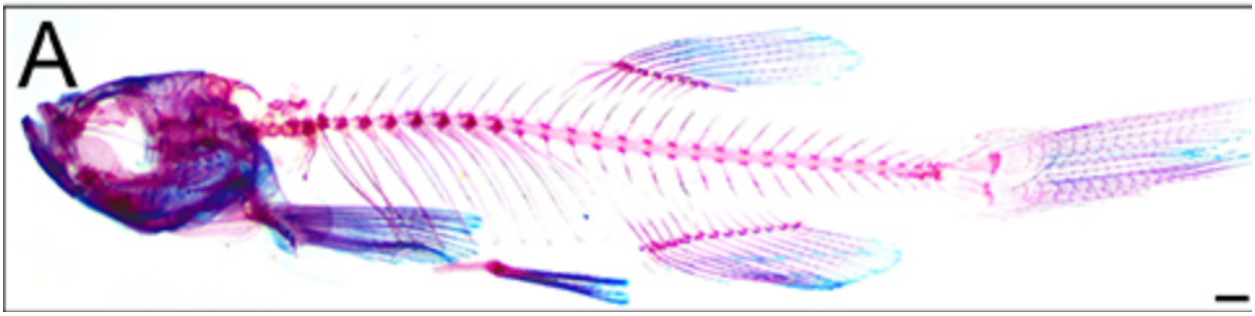

Figure 1. A zebrafish skeleton stained to show bone in red and cartilage in blue. Image from (Bergen et al., 2019)

Because age is not indicative of development stage due to differences in rearing densities and temperature that can affect the speed of development (Parichy et al., 2009), stages of zebrafish development are tracked using fish size rather than age. The method of measuring zebrafish size is by measuring the length of the fish. Researchers measure either standard length (SL) or notochord length (NL). The anterior most point in both SL and NL measurements is the furthest most point of the jaw (whether it be the maxilla or mandible) (Bird & Mabee, 2003; Parichy et al., 2009). In NL, measurements end at the posterior point of the notochord (Bird & Mabee, 2003; Parichy et al., 2009). During development the notochord undergoes flexion, which causes a bend in the notochord (Parichy et al., 2009). Due to this, NL is not sufficient to measure zebrafish at older larval stages when flexion has occurred, starting ~4.5mm SL. SL measures to the base of the caudal fin, or more specifically the cartilages and bones (i.e. the hypurals) which support the fin rays (Bird & Mabee, 2003; Parichy et al., 2009). Measuring from the tip of the snout to the hypurals gives the SL of a zebrafish, and is the measurement used during this study.

1.5 Caudal Fin

The caudal fin, also known as the tail, is a part of the axial skeleton of the fish. It is bi-lobed and composed of several different bones: five hypurals (Hy), the parhypural (Phy), a pair of uroneurals, preural vertebrae, one epural, and a urostyle (Us) (composed of a preural centrum, ural centra, uroneurals, as well as the pleurostyle (Pl) (Bird & Mabee, 2003). Figure 2 shows a schematic of these elements. The caudal fin rays are also a part of the tail, as they are supported by the hypurals and parhypural, but are not a focus of this study (Bird & Mabee, 2003). There is a distinct lack of research on the detailed histology of the process of ossification in zebrafish (Bird & Mabee, 2003). This study focuses on the tail since the skeletal elements are flat and therefore it is easier to analyse changes in histology over development, without having to

consider curvatures in skeletal elements. While there is information on the timing of when condensations form, and when ossification occurs in the zebrafish tail (Bird & Mabee, 2003; Jeradi & Franz-Odendaal, 2022), the changes to the cells during this process has not yet been recorded. The focus of this study are the five hypurals and the parhypural of the zebrafish tail.

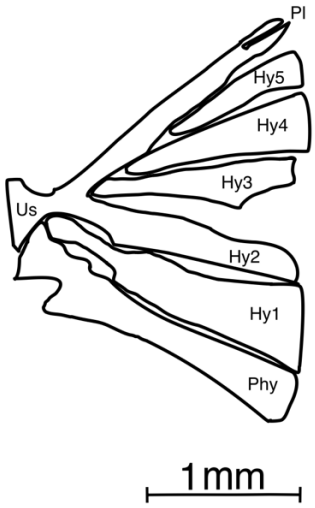

Figure 2. Schematic of the caudal fin bones of a 28 mm SL zebrafish. Terminology: Us, urostyle (Pl, pleurostyle a part of the urostyle); Hypurals, Hy (1-5); Phy, Parhypural. Figure redrawn from Wiley et al., 2015.

The hypurals are laterally flattened cartilaginous elements of the preural vertebrae (i.e. the hemal arches and spines), which support the jointed fin rays of the tail (Bird & Mabee, 2003). The parhypural is a part of the hemal arch and spine of the preural centrum (Bird & Mabee, 2003). Hypurals 1 and 2, along with the parhypural, support the lower lobe of the caudal fin, while hypurals 3 to 5 support the upper lobe (Bird & Mabee, 2003). The timing of development of the hypurals and the parhypural have been studied and are shown in Table 1 as well as mapped out graphically in Figure 3 (Bird & Mabee, 2003; Jeradi & Franz-Odendaal, 2022) . While many authors have described the ossification of the hypurals and parhypural to be

endochondral (Jeradi & Franz-Odendaal, 2022; Weigele & Franz-Odendaal, 2016), others have indicated that the mode of ossification is perichondral (Bensimon-Brito et al., 2012).

Table 1 - Timing (using size) of different skeletal development processes in the caudal fin in SL.

Element	Condensation formation	Ossification onset	Fully formed bone
Hypural 1	3.8 mm	5.0 mm	5.1 mm
Hypural 2	4.0 mm	5.0 mm	5.2 mm
Hypural 3	4.4 mm	5.0 mm	5.1 mm
Hypural 4	4.8 mm	5.1 mm	5.1-5.6 mm
Hypural 5	5.0 mm	6.2 mm	6.3 mm
Parhypural	3.8 mm	5.2 mm	5.3 mm

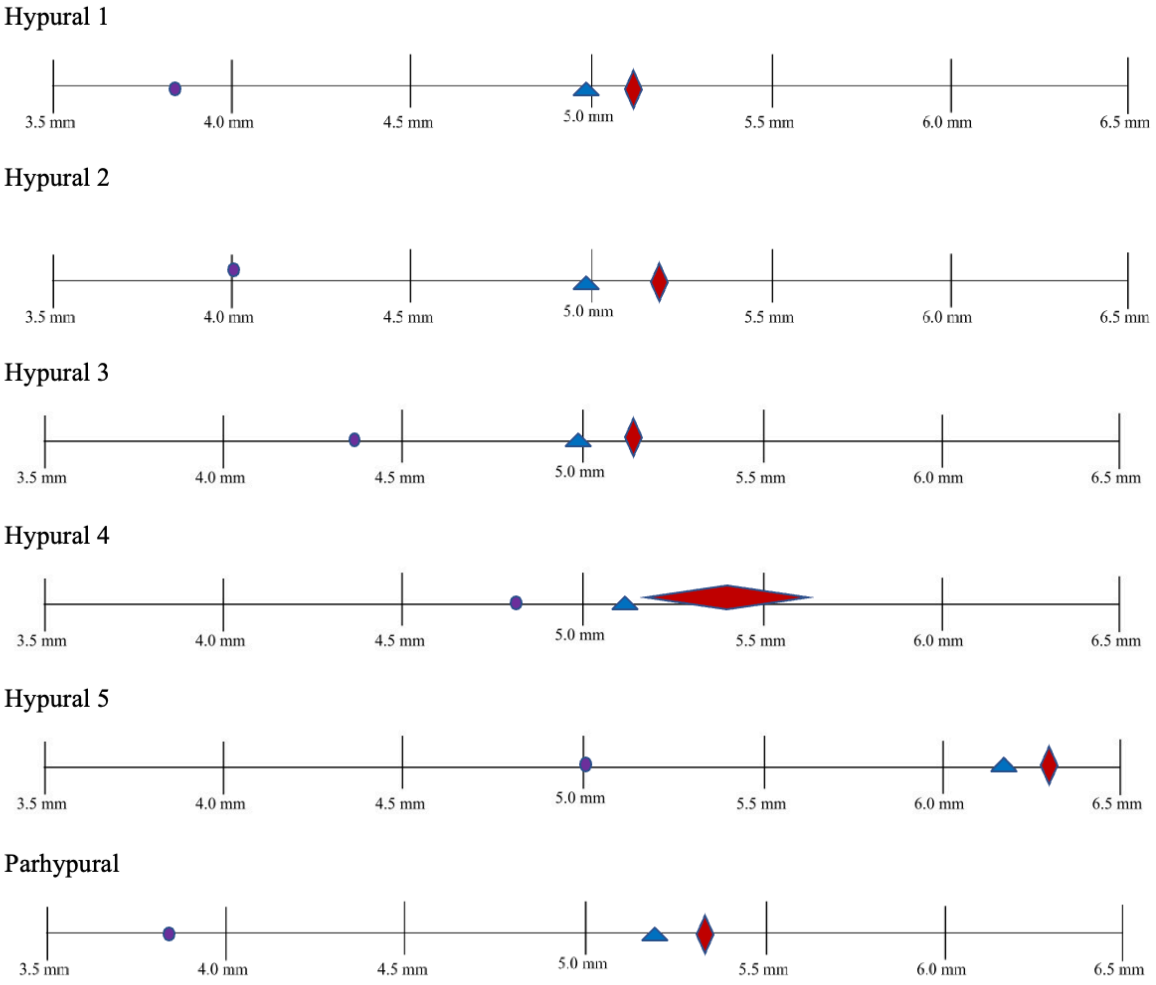

Figure 3. Timelines of ossification in the five hypurals and the parhypural**.** Purple dots indicate the earliest presence of the condensation, blue triangles indicate earliest ossification onset, and red diamonds indicate the first presence of fully formed bone. Hypural 4 has a long range in which fully formed bone could be present, with the left tip being the earliest found fully formed bone. Data from Bird & Mabee, 2003; Jeradi & Franz-Odendaal, 2022 .

1.6 Significance of this Research

This study provides information on the detailed process of endochondral ossification in zebrafish, and is relevant to many other organisms, including humans. Already there are studies investigating how zebrafish bone regenerates, and how the findings could be applied to humans (e.g. Dietrich et al., 2021; Rolland-Lagan et al., 2012; Tonelli et al., 2020). This thesis study will help to fill the knowledge gap of the histology of endochondral ossification, as well as improve

our understanding of the zebrafish skeletal biology. The primary objectives are to investigate the changes in the morphology of the cells, and cartilage template over time in the hypurals and parhypural of the zebrafish. My hypothesis, based on the literature of endochondral ossification, is that the rate of endochondral ossification will be different for the hypurals, but the morphological changes to the cells will be the same for the six elements. I predict that the cartilaginous matrix will decrease in area over time as it is replaced by bone. I also predict that the area of the cells will increase as a result of the change from chondrocytes to hypertrophied chondrocytes, and later decrease as osteoblasts differentiate to osteocytes. Furthermore, I expect endochondral ossification to occur from within the cartilage template, rather than from the outside in (as in perichondral ossification), due to it being the mode of ossification most as described by most authors.

2 Methods

2.1 Zebrafish husbandry

2.1.1Ethics statement

The zebrafish were handled following the SMU-MSVU Animal Care Committee protocol (protocol #21-09A2), which approved the work outlined in this thesis. Live zebrafish were handled by other members of the Franz-Odendaal Bone Development Lab, who are certified to handle zebrafish.

2.1.2 Measurements of zebrafish body length

To measure the length of the zebrafish (post-fixation), they were placed into a petri dish and measured in standard length (SL) using a dissecting microscope and a ruler. SL measures from the tip of the snout to the base of the cartilages and bones (i.e. the hypurals) which support the fin rays (Bird & Mabee, 2003; Parichy et al., 2009).

2.1.3 Growth conditions of zebrafish

The MSVU standard operating procedures for rearing fish was followed throughout fish rearing and collection. Zebrafish from the wildtype AB strain were provided by Dalhousie University. Twenty fish were grown in the same rearing cup for the first 4 days after fertilization, after which the fish were split into 2-3 separate rearing cups, with a total of 27 samples used overall in this study. Fish were reared at MSVU by members of the lab until they reached the desired sizes, namely, ~4.5 – 9 mm SL. From 0 – 4 dpf, the fish were kept in cups with ~1 inch of water. From 4 – 30 dpf the fish were in cups with ~250mL of water. The water was at a temperature range of 26 – 28^{o}C, with a pH of 7.0 – 7.4 and a salinity of 600 – 700µS. There was a controlled photoperiod with lights being turned on at 7:00 AM and turned off at 7:00PM. Fish were fed three times each day, with either Gemma 75 for fish 5 – 17 dpf, or with Gemma 150 for fish greater than 17 dpf.

Fish were euthanized by placing them in a lethal dose of buffered MS222 (Tricaine). All samples were fixed by placing them in 4% paraformaldehyde (PFA) overnight and then storing them in phosphate-buffered saline 1XPBS (see Appendix B and C for recipe and chemical information). All transfers of fish between solutions were done using plastic pipettes.

2.1.4 Samples

A total of 27 zebrafish were used during the study, however only nine samples had the parhypural and hypurals present, and were subsequently measured. These nine samples were put into three distinct groups based on body length (Table 2).

Table 2 – Sample length and sample size categorized by group

Group	Fish length (mm SL)	Sample size
	~4.5	1
1	5	3
	5.5	1
	6	1
2	7	1
	8	1
3	9	1

2.2 Histology

2.2.1 Embedding samples into wax

Samples were placed into a tube with a lid, and enough ethanol was put in the tube to fully cover the fish. The samples were processed through a series of ethanol solutions starting from 25% ethanol, and going through: 50%, 70%, 80% and 90%, at 45-minute intervals. At 70% ethanol, the samples were left overnight before continuing the ethanol series the next day, going back to 45-minute intervals for 80 and 90% ethanol. After the 90% ethanol was removed, 100% ethanol was put into the tube for an hour and then repeated a second time. The samples were then placed into citrosolve for an hour, before citrosolve was removed and fresh citrosolve was placed into the tube for one more hour. These steps were used to dehydrate the samples. A pipette was used to remove the solutions from the tubes before adding in the next solution. Metal embedding trays were filled with low-melting point paraffin wax, which was melted in a VWR oven set at 62^{o}C. The samples were then removed from the tubes using a pipette, and placed on a kimwipe to pat dry. The samples were then placed carefully into an embedding tray, ensuring that the fish was in a straight position without any bends in the body, before being placed into a Napco model 5831 vacuum oven overnight, with the pressure set between 19 and 20 hg. The next day, the samples were transferred to another container for two more hours in the vacuum oven set to the same pressure and temperature as previously stated. The samples were removed from the

vacuum oven and placed into smaller embedding trays in the VWR oven with molten paraffin wax in them and placed in the same orientation, as shown in Figure 4. The samples were orientated so that they would be sectioned laterally from left to right, allowing for the sectioning to be parallel to the caudal fin. The containers were placed on an ice pack and any necessary adjustments to orientation were made. A white cartridge was placed on top of the smaller container and wax was poured into the tray until it reached the top of the white cartridge. The blocks were left on the ice pack for about an hour to ensure that the specimen would not move if the block was moved, before being placed into a freezer overnight.

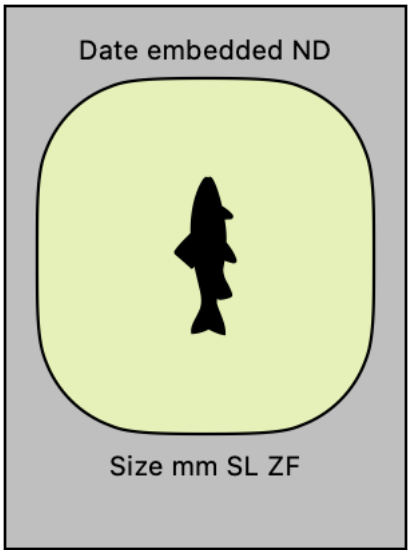

Figure 4. Example of an embedded zebrafish showing orientation. The gray indicates the white cartridge that was labelled.

2.2.2 Sectioning

Microscope slides were labelled with the fish SL size and the day it was sectioned, along with the section thickness and placed onto a slide warmer to help warm water that was placed onto the slides to have the sections stick to the slides. Using a Leitz 1512 microtome samples were sliced in sagittal sections. Samples were initially sectioned at 5 µm, however during data collection this changed to 6 µm sections instead, to improve section integrity. The sections were then placed onto the prepared slides with warm water on them in order to allow them to expand

and to remove wrinkles. The water was drained carefully using a kimwipe and the slides were kept in a Labnet mini-incubator set at 37^{o}C overnight.

2.3 Stains

2.3.1 Hall Brunt Quadruple stain

Sections were stained using the Hall Brunt Quadruple stain (HBQ stain) to stain bone red and cartilage blue, following the procedures laid out in Hall (1986) with optimizations from the Bone Development Lab (Hall, 1986). The full optimized protocol is provided in Appendix A, along with a list of all stains used. These optimizations include using two rounds of citrosolve washes for 5 minutes each before beginning the hydration ethanol series from 100 % to 50%. Starting with 100% ethanol twice, and a single change to 90%, 70% and ending with 50%. Next was a rinse in distilled water for 2 minutes to finish the re-hydration procedure before staining. The same stains were used as in Hall (1986), with the timings for rinses of the slides post-stain changed to 1 minute in distilled water after all stains except Celestine Blue (from Sigma Aldrich) and Direct Red (from Sigma Aldrich). After Celestine Blue, the slides were rinsed for 2 minutes, and after Direct Red, the slides were rinsed for 20 seconds. The slides were then dehydrated in two changes of 100% ethanol for 20 seconds each before clearing the slides. To clear the slides, they were placed into citrosolve for 1 minute repeated four times. Following this, 2-3 drops of DPX mountant (Sigma Aldrich; 06522) were placed onto the slides and a coverslip carefully was placed on top.

2.3.2 Masson's trichrome staining

Masson's trichrome staining was used alongside the HBQ stain to stain type I collagen a dark green. The full protocol is provided in Appendix A. The same method for clearing the wax from the sample was used during this procedure as was used for HBQ staining. An optimized version of the staining procedure (each stain from Sigma Aldrich) has been previously developed in the Franz-Odendaal Bone Development Lab and is as follows: submerge in Mayer's

hematoxylin for 10 minutes, Scott's tap water for 30 seconds, xylidine ponceau for 2 minutes, phosphomolybdic acid for 4 minutes and light green for 90 seconds. After each stain dip the slides in distilled water to rinse before putting it into the next one. After the rinsing from light green, dip in 100% ethanol twice. Slides were cleared in the same manner as for the HBQ stain and 2-3 drops of DPX mountant were put onto the slides before placing a coverslip on top.

2.4 Data Analysis

2.4.1 Slide imaging

Slides were observed using a Nikon eclipse 50i microscope. Images of the slides were taken with a Nikon DS-Fi2 camera, which attaches to the microscope, at 20x magnification. The imaging software NIS-Elements BR was used to capture the images.

Schematics of the zebrafish tail were created from images in Wiley et al. (2015) as shown in Figure 2 and were printed out and then coloured in manually to show the amount of cartilage and bone present on all slides made for each sample, using each section to determine all areas with bone and cartilage. This was done using blue, red, pink, purple and green crayons. Following colouration of the schematics, the hypurals within all samples were compared. Using both the morphology of the cells and the results of the stain, bone was coloured red, and cartilage was coloured blue. These schematics have been included in Appendix D, E and F.

2.4.2 Grouping

On the schematics for these three groups (Appendix D, E, and F) it was found that the majority of the data set had hypurals 2 and 3 present. Not all samples had both elements, with one sample from groups 1 and 2 missing hypural 2, as well as hypural 3. However the samples that were missing hypural 2 were not the same samples that were missing hypural 3. The reason why some sections don't have all the hypurals is either due to small angle differences in the plane of the sections or the cartilage templates of the elements had not formed yet.

2.4.3 Hypural measurements

Using the software mentioned in 2.4.1, several measurements were taken from the images taken at 20x magnification. Using the same software, the total lengths of the hypurals were taken, measuring the distance from the proximal most point to the distal point in the middle of the elements (Figure 5). A second measurement was taken of the length of the zone of flattened chondrocyte, the chondrocytes that have not yet undergone hypertrophy, from the middle of the element to determine what percentage of the hypural has not yet undergone hypertrophy (Figure 5). The hypurals measured were chosen following the results of the analysis of the coloured in schematics as discussed in section 2.4.2. The measurements were taken for all slides that contained hypurals 2 and 3 and the sections with the longest element of interest were chosen.

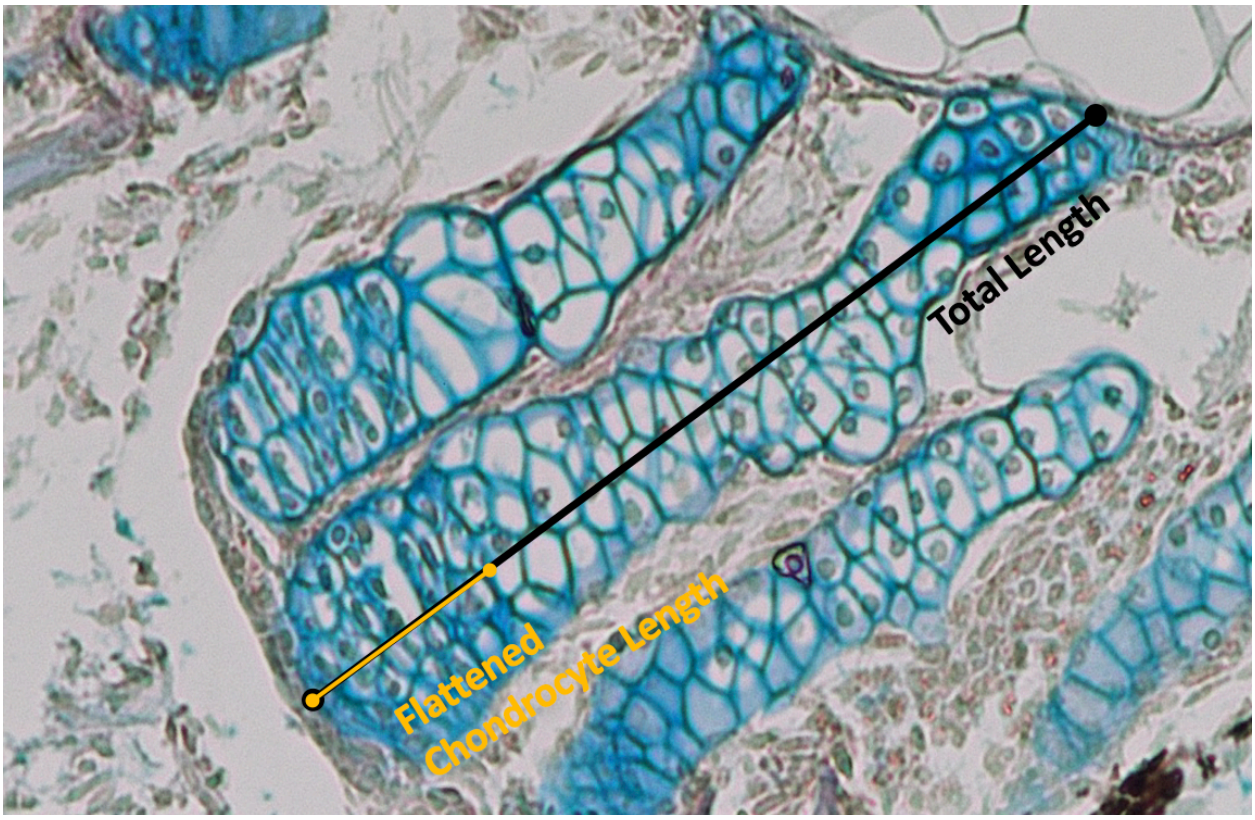

Figure 5. Example of how measurements of hypurals were taken. Black indicates total length measurement (maximum length of the hypural), yellow indicates flattened chondrocyte measurement (zone of flattened chondrocytes), demonstrated on hypural 4 of a 5 mm SL zebrafish.

A scatterplot was made for both hypurals comparing total length of the hypural to the zebrafish size (mm SL) with a line of best fit. The line of best fit's slope was calculated and used to determine growth rate. A second scatterplot comparing the total length of each hypural to the percentage of length that is occupied by the zone of flattened chondrocytes, which was determined by dividing the flattened chondrocyte length by the total hypural length and multiplying by 100. A Bar graph was created to show the mean total hypural length for the three groups.

2.4.4 Statistics

All collected data was organized and saved as a csv. file and imported into the statistical program R (R Core Team, 2022). The first step conducted was to test for normality using the Shapiro-Wilk test to determine if data was normal. Data that resulted with a *p-value* < 0.05 was determined to not be normally distributed. For p-values > 0.05, histograms were created to check for any skew within the data.

Two different outlier tests were used. Grubb's outlier test was used to check for any outliers within all normal data, using the Outliers package in R (Komsta, L, 2022). So long as the Grubb's value calculated was lower than the critical Grubb's value the data was considered to not be an outlier. This was done by installing the "outliers" package into R and running a Grubb's test, testing both the highest value in the data, as well as the lowest value. For non-normal data, a percentile approach was taken. The quantile function in R was used to create a lower bound set for the 1 percentile, as well as an upper bound for the 99 percentile. The "which" function in R was used to check for any values that fell outside of the lower and upper bounds, these values were labelled as potential outliers.

Kruskal-Wallis tests were implemented in R to check for statistical significance. Initially an ANOVA and Tukey's test was going to be used, however after implementing multiple

transformations to the raw data the normalized requirements to conduct an ANOVA and Tukey's test were not met.

2.4.5 Outliers

The total length of hypural 2 had no outliers for its highest value (G = 2.39998, *p-value* = 0.05213) and for its lowest value (G = 1.13182, *p-value* = 1). The total length of hypural 3 had no outliers for its highest value (G = 1.83836, *p-value* = 0.3966 using the Grubb's outlier test. The Grubb's outlier test also had no outliers for the lowest value of the total length of hypural 3 (G = 1.48982, *p-value* = 0.9515). So long as the data was between the two Grubb's outlier test values, they were considered to not be an outlier. However, much like ANOVA testing, the Grubb's outlier test requires for data to be normal, so a second outlier test was conducted for non-parametric data.

Outliers were tested in non-normal data by using percentiles. There were four potential outliers found using the percentiles as shown in Table 3. To determine whether any of the potential outliers would have a strong effect on the data, a comparison of the highest and lowest non-outlier values for each data point was made. A potential outlier for the flattened chondrocyte length (μm) of hypural 2 had a value of 54.35 μm. The highest non-outlier value was 54.26 μm. Both of these values were from samples within group 3. This is close enough to the potential outlier that it was determined that the measurements for the zone of flattened chondrocyte of hypural 2 was not an outlier. The ratio of flattened chondrocytes to total length for hypural 2 had a potential outlier of 40% in group 1. The closest value to this was 34% in group 1. This falls close enough that this value should not skew the data. For hypural 3, the flattened chondrocyte length had a potential outlier value of 89.75 μm, and the ratio of flattened chondrocyte length to total length had a potential outlier value of 49%. These values both came from the same sample

in group 2, and were the only potential outliers that were from the same sample. When compared to the other values within group 2 for all samples, the flattened chondrocyte length is 32.39 µm longer than the highest non-outlier value. This is quite the gap, indicating that this value may be skewing the data. The flattened chondrocyte to total length ratio had a highest non-outlier value of 44%. The measurements from this section were removed due to being an outlier, removing the 89.75 µm flattened chondrocyte length and the 49% values from the data set. The results of the outlier testing caused the data points of 89.75 µm and 49.13% to be removed from the 6 mm SL zebrafish specimen.

Table 3 – Percentile boundaries for potential outliers in non-parametric data.

	Lower Bound (1%)	**Upper Bound (99%)**	**Potential outlier**	**Highest value in dataset**
Hypural 2 flattened chondrocyte length (µm)	0	54.3374	54.35	54.26
Hypural 2 percentage of flattened chondrocytes	0	40.14%	40.62%	34%
Hypural 3 flattened chondrocyte length (µm)	0	85.2154	89.75	57.36
Hypural 3 percentage of flattened chondrocytes	0	48.53%	49.13%	44%

2.5 Issues during data collection

Throughout data collection several issues arose that affected the data collected. These problems included orientation issues of the samples during the embedding protocol, which resulted in no hypurals and parhypurals in the sections. In a few samples, the incorrect

orientation of the fish did not affect the tail, for those samples data was able to be collected. To fix this orientation issue pre-embedding the samples in agarose was investigated. It was found that pre-embedding the sample did not help with any orientation issues. To mitigate the orientation issue, embedding was done very carefully to ensure fish would stay in the correct orientation within the wax block.

One issue that could not be fixed was that the intensity of the stains differed for each round of staining conducted. There were some samples that stained very lightly, while others stained darkly. Another issue with the staining that occurred during data collection was that some samples stained unexpectedly. The 6 mm SL zebrafish in group 2 had cartilages staining differently than expected using HBQ. This sample stained the tail cartilages a purple colour and the head cartilages red, rather than the expected blue. The differences in staining intensity could be due to rinse length differences (e.g. a few seconds difference can affect the stain intensity). Another factor that could lead to differential staining intensity is any cross-contamination of the stains by ethanol and/or water by others in the laboratory.

The third issue that may have caused errors within the results were issues with sectioning. The hypurals and parhypural of some samples were not visible in the sections. This could be due to section collection beginning too late, thus missing the area of interest. Another issue with sectioning was that the section ribbons would sometimes split down the middle. Some of these splits created sections that could not be used because the splitting separated the elements of interest from the rest of the body, or tor the elements of interest. This made identification of the hypurals and parhypural difficult resulting in some unidentified hypurals. This splitting is a result of a defect (e.g. a nick) in the sectioning knife. One more potential issue with sectioning is that

the angle of specimen may have resulted in the entire hypural to not be properly represented. Angle issues may have resulted in only parts of the hypural being present.

One final potential issue to note is the change in sectioning thickness. Section thickness was changed from 5µm to 6 µm due to more efficient sectioning. This change limited the number of chondrocytes that could be counted and measured.

3 Results

3.1 Descriptive characteristics of hypural ossification

Using the schematics (Appendix D, E, F) and all slides created for each individual sample, descriptions of the caudal fin histology are explained here. Each explanation has a cumulative representation of the overall ossification process for each age group, so figures do not represent all findings for each sample, but are still representative of the histology.

3.1.1 Group 1 (4.0 mm SL to 5.49 mm SL, n = 4)

The youngest group studied had limited to no bone formation in the tail (Figure 6, Appendix D). In the earliest stage (around 4.5 mm SL) the cartilaginous model was still forming, and no ossification was observed (Figure 6a). This sample only has the first and second hypurals and the parhypural visible. This sample has a very light stain with HBQ, with elements staining an unusual pink colour. The first of the 5 mm SL zebrafish has no ossification present. There was evidence of chondrocytes hypertrophying in the middle of the hypural, with both the proximal and distal tips having flattened chondrocytes rather than hypertrophied chondrocytes (Figure 6b). The first 5 mm SL sample contains hypurals 2 to 5, all of which have a blue stain, again with no ossification present. The second 5 mm SL zebrafish contains hypural 2 and 3 (Figure 6c). For the most part, the elements within this fish are cartilaginous. This sample has hypertrophy both proximally and medially, with flattened chondrocytes in the distal tip (Figure 6c). The final sample within this group does have some indication of bone formation on hypurals 2 to 5 (Figure

6d). Specifically, hypurals 4 and 5 have a red stain perichondrally, while hypurals 2 and 3 have some red staining on the distal tips of the hypurals (Figure 6d). This sample also has hypertrophied chondrocytes medially, and flattened chondrocytes within the proximal and distal tips (Figure 6d).

In summary, the onset of ossification was only visible in a quarter of the samples analysed in this group. This was observed in hypurals 2 to 5 to different degrees, and indicates that ossification of the tail has just begun. Interestingly, all samples have zones of hypertrophic and flattened chondrocytes, which is indicative of the phase just prior to ossification (presence of bone).

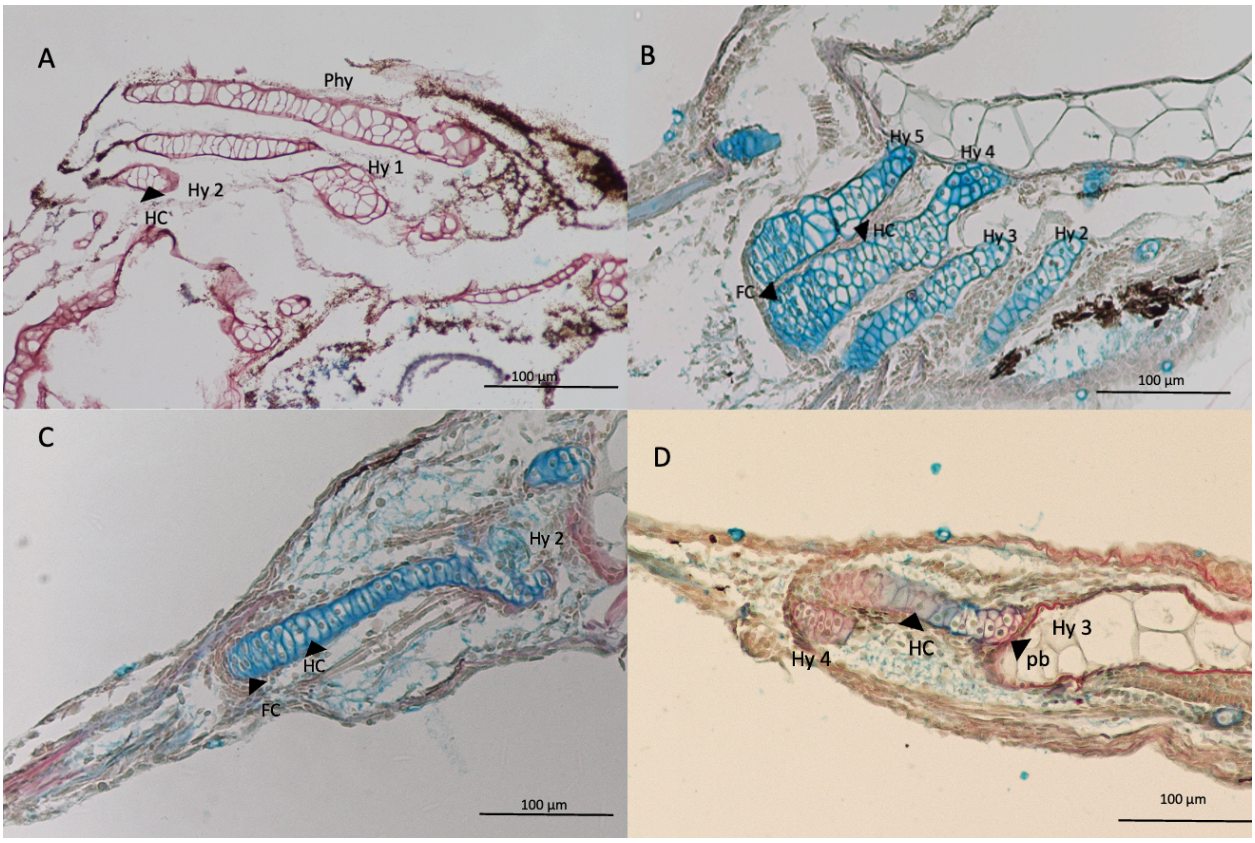

Figure 6. Annotated images of HBQ stained caudal fin of group 1 larval zebrafish. Cartilage is stained blue while bone is red. A) 4.5 mm SL zebrafish, stained pink instead of the expected blue for cartilage. B) 5 mm SL zebrafish; cartilage is present, and chondrocytes have undergone hypertrophy in the middle of the elements with flattened chondrocytes on one end of the element (Hy 2 to Hy 5). C) 5 mm SL zebrafish, hypural 2 with both hypertrophied and flattened chondrocytes. D) 5 mm SL zebrafish, hypural 3 and 4, some potential bone ossification may have resulted in red staining on proximal and distal tips of hypural 3. The distal end is towards the left of each image. HC = hypertrophied chondrocytes, FC = flattened chondrocytes, pb = potential bone or ossification, Hy = hypural, Phy = parhypural.

3.1.2 Group 2 (5.5 mm SL to 7.5 mm SL, n = 3)

The middle group (5.5 to 7.5 mm SL) investigated in the larval zebrafish has the beginning of bone ossification within all three samples (Figure 7). The smallest sample (5.5 mm SL) appears to have red staining along the edges of two hypurals, indicative of perichondral ossification (Figure 7a). It is not clear which hypurals are present, however using the morphology of the elements and their location, it is likely that these elements are hypurals 3 and 4. This sample does have (a region of) flattened chondrocytes at the distal tips of the elements although they are not

very prevalent in all slides. The 6 mm SL zebrafish has the parhypural and hypurals 1 to 4 when looking at all slides in the sample (Figure 7b). All elements, except hypural 4, have a red edge indicating bone ossification has begun in the others, but has not yet begun for hypural 4 (see Appendix E for hypural 3 and 4, Figure 7b displays the parhypural and hypural 1 and 2). The red staining is present perichondrally, however hypural 3 does have some red staining on the distal tip of the element (Appendix E). All flattened chondrocytes are located distally on this sample (Figure 7b). The 7 mm SL sample has all six elements, with each element having bone ossification on the edges of the elements (Figure 7c). The edges of the elements in this sample are not completely red, with gaps towards the distal tips for most elements (denoted by the asterisk on Figure 7c). The Masson's trichrome stained 7 mm SL slide (not shown in Figure 7) confirms that bone is forming, with a dark green edge on all six elements (Appendix E). No flattened chondrocytes are present within any of the hypurals or parhypural in this sample, indicating that all chondrocytes are hypertrophied (Figure 7c).

In summary, in this group of fish (5.5 to 7.5 mm SL), bone has begun to develop perichondrally, forming bone edges with no interior bone formed. This was observed within the parhypural and the five hypurals. There are few flattened chondrocytes indicating that most have undergone hypertrophy within this group by the largest sample within the group.

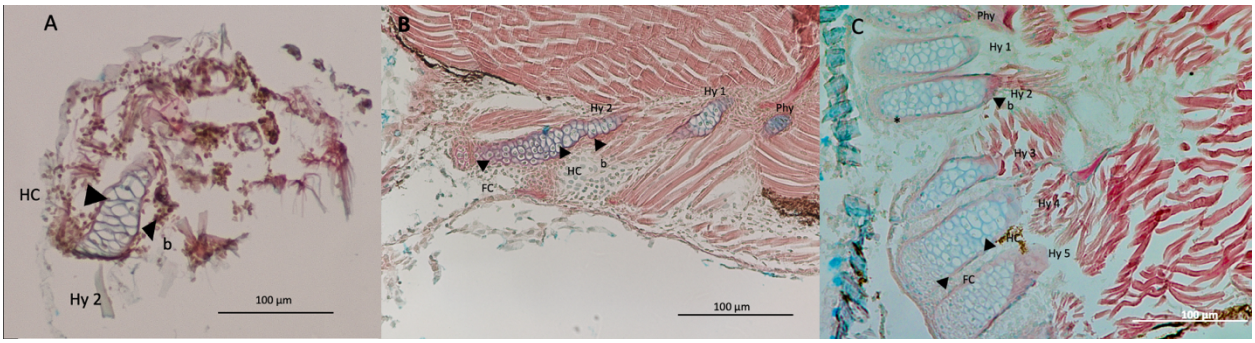

Figure 7. Annotated photos of HBQ stained caudal fin of group 2 larval zebrafish. Cartilage is stained blue while bone is red. A) 5.5 mm SL zebrafish, hypural 2 has hypertrophied chondrocytes and bone present. B) 6 mm SL zebrafish, hypurals 1 and 2 and the parhypural have both hypertrophied and flattened chondrocytes with bone present on the edges. C) 7 mm SL zebrafish, very lightly stained all six elements are present with hypertrophied chondrocytes and flattened chondrocytes, a red stained edge indicates that bone has ossified. The distal end is towards the left of each image. HC = hypertrophied chondrocytes, FC = flattened chondrocytes, b = bone, Hy = hypural, Phy = parhypural, * = non-red edge of the 7 mm SL zebrafish.

3.1.3 Group 3 (8 mm SL to 9.5 mm SL, n = 2)

The third group of larval zebrafish studied has bone formation in the hypurals and parhypural of the caudal fin, with most of the edges red (Figure 8, Appendix F). The 8 mm SL zebrafish has all of the hypurals visible within the stained slides. In this sample the proximal tips of hypurals 4 and 5 are red, indicating that bone is forming (Figure 8a). There is some red stain in hypurals 2 and 3 however the stain intensity is very light. For HBQ, the distal tips and edges of the zebrafish still retain the blue staining, indicating chondrocytes only and no bone formation. This sample has flattened chondrocytes within the distal tips of all the elements (Figure 8a). By 9 mm SL, the larvae have clear ossification on all elements (Figure 8b). All six elements are present within the sample. The red edges prominent in all sections indicates that ossification has indeed proceeded further at this last stage than in earlier stages (Figure 8b). The red surrounds the majority of each element, with the cartilaginous model remaining in the middle and distal tips of the parhypural and hypurals. This sample has flattened chondrocytes distally, with the presence of flattened chondrocytes proximally on one slide (Figure 8b).

In summary, for the 8 to 9.5 mm SL group, ossification has proceeded in all elements, continuing the perichondral bone development. Bone has developed towards the proximal tips of the elements but has not yet formed towards the distal tips. Flattened chondrocytes are present distally in most elements.

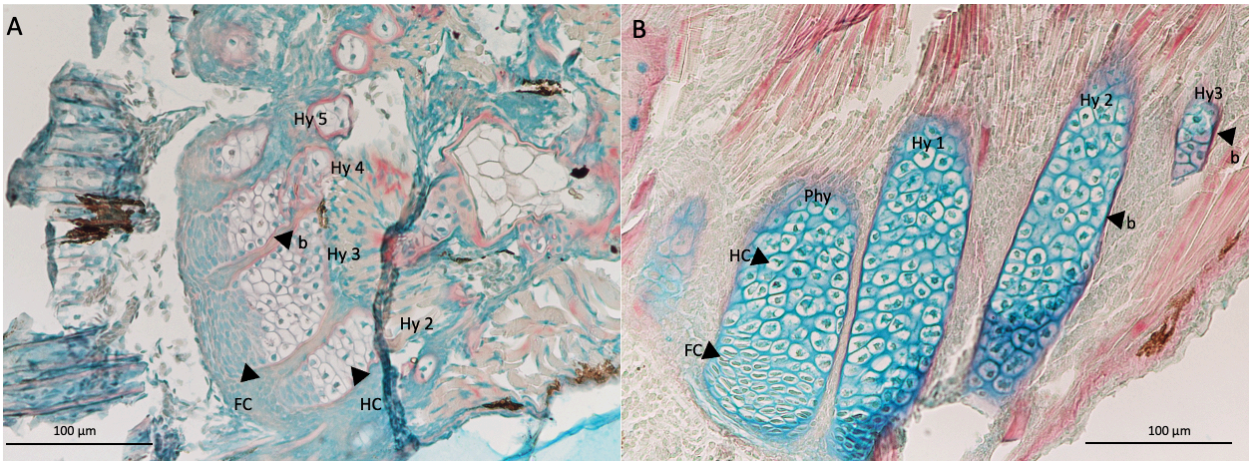

Figure 8. Annotated photos of HBQ stained caudal fin of group 3 larval zebrafish. Cartilage is stained blue while bone is red. A) 8 mm SL zebrafish, hypurals 2 to 5 are present with hypertrophied and flattened chondrocytes and a perichondrally-formed bone. B) 9 mm SL zebrafish, both cartilage and bone present with bone having developed perichondrally, some hypertrophied chondrocytes in the elements (Phy, and Hy 1 to Hy 3), the unlabelled element next to the parhypural is the hemal spine of the preural vertebrae (not focused on in this study). The distal end is towards the left of A and the bottom of B. HC = hypertrophied chondrocytes, FC = flattened chondrocytes, b = bone, Hy = hypural, Phy = parhypural.

3.2 Hypural 2 quantitative measurements

3.2.1 Normality

The Shapiro-Wilk test shows that hypural 2 has a normal distribution for the total hypural length (W= 0.88213, p-value = 0.05105). Hypural 2 is not normally distributed for flattened chondrocyte length (W = 0.81889, p-value = 0.006492), nor for the ratio of flattened chondrocytes to total length (W = 0.84206, p-value = 0.01343).

Total length for hypural 2 has a normal distribution with no skew, shown by the histogram created (see Appendix G).

3.2.2 Growth over time

There is a general increase in total hypural size over time for hypural 2 (Figure 9). The length of the hypural 2 changes from 90.1 µm (±45.7) in the smallest group to 154.3 µm (±101.1) in the largest size group (Appendix H). Hypural 2 has a growth rate of 23.38 µm per mm SL grown (Figure 9). Hypural 2 has a small increase in average total length going from 90.1 (±45.7 µm, n = 4) in group 1 to 105.2 (±14.0 µm, n = 2) in group 2. There is a far larger increase between group 2 and group 3 with an increase of 49.1 µm to have an average total length of 154.3 (±101.1 µm, n = 2) in group 3. There is no significant difference in hypural 2 length between groups (Kruskal-Wallis test, Chi = 1.22, p = 0.5434, df =2). This indicates that hypural 2 is increasing in length as the tail develops in larval zebrafish, but the increase is not significant. This lack of significance is due to the large variation between minimum and maximum lengths measured.

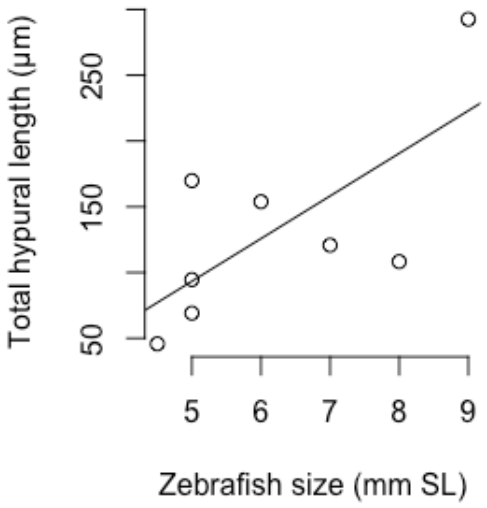

Figure 9. Total length change over time in hypural 2 total length. Line of best fit shown has a slope of 23.38.

3.2.3 Ratio of flattened chondrocytes to total hypural length

The morphological changes of the chondrocytes have an interesting pattern, with a higher percentage of flattened chondrocytes in the youngest and oldest groups for hypural 2 (Table 4). There is no significant difference in the ratio of flattened chondrocytes to total hypural length between the three groups (Kruskal-Wallis test, Chi square = 0.54933, p = 0.7598, df= 2). There may be other factors causing the percentage of flattened chondrocytes to increase for the oldest group. The mean ratios of flattened chondrocytes to total length is likely highly impacted by the 0% data points in each group.

In summary for hypural 2, there is no relationship between percentage of flattened or hypertrophic chondrocytes and length of the element over developmental time (i.e. by group). There is a maximum of 42% of flattened chondrocytes in any group.

Table 4 – Mean total length and mean flattened chondrocyte percentage of hypural 2 by group

	Hypural 2					
Group	**Mean total length (µm)**	**Standard deviation**	**Mean flattened chondrocyte length**	**Standard deviation**	**Mean flattened chondrocyte %**	**Standard deviation**
1	90.11	45.70	17.31	16.85	23%	0.18
2	105.23	13.99	13.80	23.37	18%	0.25
3	154.28	101.14	36.96	24.14	27%	0.04

3.3 Hypural 3 quantitative measurements

3.3.1 Normality

Hypural 3 has similar findings for the Shapiro-Wilk test as hypural 2, with the total hypural length having normal distribution (W = 0.89319, p-value = 0.07494) and non-normal distribution for flattened chondrocyte length (W = 0.85909, p-value = 0.02342) and the ratio of flattened chondrocytes to total length (W= 0.87029, p-value = 0.03407). The histogram for total length for hypural 3 shows heavy negative-skew (Appendix G). A log transformation was therefore used to normalize the data for total length of hypural 3.

3.3.2 Growth over time

There is a general increase in total hypural size over time for hypural 3 (Figure 10). The length of the hypural 3 changes from 125.1 µm (± 55.9) in the smallest group to 180.9 µm (±119.7) in the largest size group (Appendix H). Hypural 3 has a growth rate of 29.16 µm per mm SL grown (Figure 10). Group 1 has an average total length of 125.1 (± 55.9 µm, n = 2) which decreases to 113.5 (±24.6 µm, n = 3) in group 2. Hypural 3 then increases in size for group 3 with an increase of 67.4 µm, for a total hypural length of 180.9 (±119.7 µm, n = 2) in group 3. Hypural 3 has no significant difference between groups for total length (Kruskal-Wallis test, Chi = 2.0952, p = 0.3508, df =2). This indicates that hypural 3 is increasing in length as the tail develops in larval zebrafish, but the increase is not significant. This lack of significance is due to the large variation between minimum and maximum lengths measured.

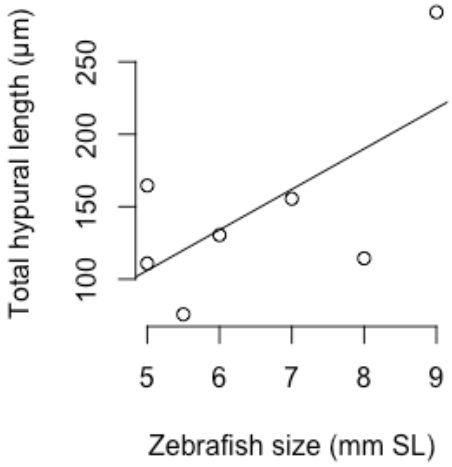

Figure 10. Total length change over time in hypural 3. Line of best fit shown with a slope of 29.16.

3.3.3 Ratio of flattened chondrocytes to total hypural length

In hypural 3, the percentage of flattened chondrocytes is higher for the youngest and oldest groups, and lowest for group 2 (Table 5). There is no significant difference for the ratio of

flattened chondrocytes to total length in hypural 3 between the groups (Kruskal-Wallis test, Chi square = 0.80192, $p = 0.6697$, df = 2) for the ratio of flattened chondrocyte length to total length. This indicates that the proportion of flattened chondrocytes increases in size (although not significantly) during development, but that there are other factors causing the percentage of non-hypertrophied chondrocytes to increase. The data is quite varied, with some samples having no zone of flattened chondrocytes and others having a large zone of flattened chondrocytes, meaning that this pattern may need future research to determine if it is a standard pattern across all zebrafish.

Table 5 – Mean total length and mean flattened chondrocyte percentage of hypural 3 groups

Hypural 3						
Groups	**Mean total length (µm)**	**Standard deviation**	**Mean flattened chondrocyte length**	**Standard deviation**	**Mean flattened chondrocyte %**	**Standard deviation**
1	125.09	55.94	14.68	17.01	18%	0.26
2	113.46	39.38	17.54	25.22	15%	0.18
3	180.97	119.71	27.01	8.18	19%	0.13

3.4 Comparison of hypural 2 and hypural 3

3.4.1Total length

Both hypurals have an overall increase in total length as the size of the fish increases. Interestingly, hypural 2 initially has more growth than hypural 3 however it is quickly over taken around 8-9 mm SL hypural 3 becomes larger than hypural 2, as shown by the larger mean total length of groups 1 and 2 for hypural 2 (Figure 11). There is no significant difference (Kruskal-Wallis test, Chi square = 0.3219, $p = 0.5705$, df = 1) between the total length of the two hypurals however.

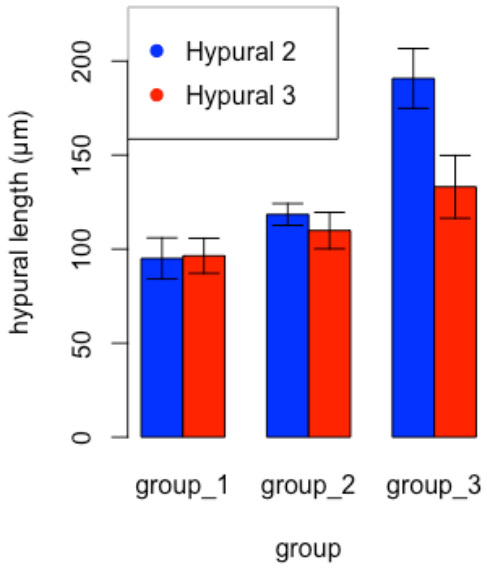

Figure 11. Mean total hypural length (µm) for each group. Group 1 (n = 4) has the smallest mean total length for hypural 3, group 2 (n = 3) has the smallest mean total length for hypural 2, while group 3 (n = 2) has the highest total length for both hypurals. Hypural 2: group 1 mean length is 90.11 (±45.70 µm), group 2 mean length is 105.23 (±13.99 µm), and group 3 mean length is 154.28 (±101.14 µm). Hypural 3: group 1 mean length is 125.09 (±55.94), group 2 mean length is 113.46 (±39.38), and group 3 mean length is180.97 (±119.71). Hypural 2 is shown by the blue bars while hypural 3 is shown by the red bars, error bars display the standard deviation from the mean length.

3.4.2 Growth rate

Both hypurals have a positive growth rate (i.e. slope of line in figure 9 and 10) of total hypural length as zebrafish size inceases. Hypural 3 has a faster growth rate on average, but hypural 2 has faster growth initially (Figure 12). When comparing the growth rate indicated by the line of best fit in Figure 12, there is a different growth rate for the two hypurals.

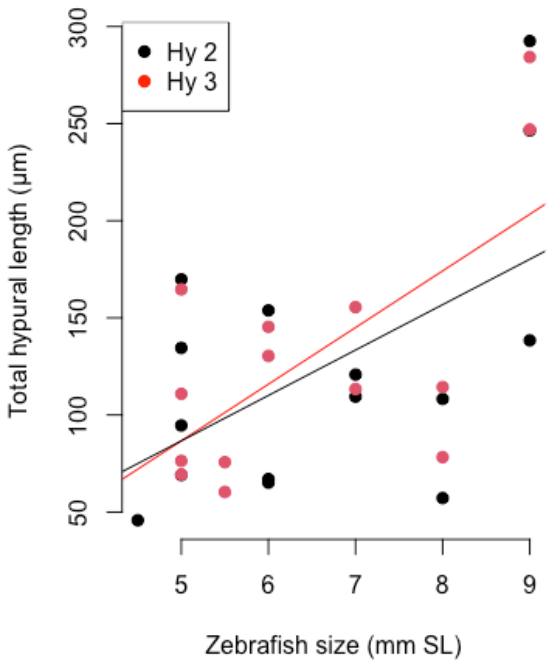

Figure 12. Scatterplot of total hypural length growth over zebrafish size SL. Black dots indicate hypural 2, with a black line of best fit showing rate. Red dots indicate hypural 3, with a red line of best fit showing rate.

3.4.3 Ratio of flattened chondrocytes

One evident pattern is the change in the amount of flattened chondrocytes. In both hypural 2 and 3, the percentage of flattened chondrocytes within the total length of the hypurals has a decrease from group 1 to group 2, and an increase from group 2 to 3 (Tables 4 and 5). This indicates that the morphological changes to the chondrocytes are similar between the elements. These changes in percentages are not significant for either hypural. It is interesting that the proportion of flattened chondrocytes remains at 18-27% of the total length of the cartilage element, and is never more than one third of the element.

4 Discussion

Two of my three predictions were confirmed through the data. The cartilaginous matrix did indeed decrease in area as the larval zebrafish developed from group 1 to group 3, shown by

the presence of bone along the edges of the latter two groups. This indicates that the mode of ossification for larval zebrafish caudal fin undergoes the process of bone replacing cartilage as expected from the literature (Bird & Mabee, 2003). The second prediction confirmed is the morphological changes to the chondrocytes did include hypertrophy. However, the perichondral growth of the bone, forming as a collar on the edges rather than from the centre, is more indicative of perichondral ossification than endochondral ossification. Therefore while some of the findings support an endochondral mode of ossification (hypertrophic chondrocytes), others (perichondral bone collar) supports a perichondral mode of ossification. I had further hypothesized that the rate of ossification would differ among the six hypurals, but that the morphological changes would be the same. The data does support the hypothesis, as growth rate differs between hypural 2 and 3, but both display the same pattern of hypertrophy.

4.1 Mode of Ossification

The development observed throughout this study is indicative of perichondral ossification. Many authors have previously described the mode of ossification as endochondral ossification(Jeradi & Franz-Odendaal, 2022; Weigele & Franz-Odendaal, 2016), and few have described it as perichondral for the studied elements (Bensimon-Brito et al., 2012). One reason for the different modes of ossification being described for the parhypural and hypurals of zebrafish, is the use of the term endochondral ossification. Some authors have described endochondral ossification as a wider range for the replacement of cartilage with bone, lumping perichondral ossification as a part of endochondral ossification (e.g. Blumer, 2021). The use of this definition of endochondral ossification could have resulted in researchers defining the mode of ossification as endochondral, even though it has characteristics of perichondral ossification.

4.2 Rate of Growth

According to Bird and Mabee condensation presence often occurs between 3.8 to 5.0 mm SL, with hypural 5 having first condensation presence around 5.0 mm SL (2003). The results of this study does show that condensation presence occurs before 5.0 mm SL, as there was cartilage present for hypural 5 in Group 1, at this age (Figure 5d). The other five elements do appear to follow the initial condensation presence as mentioned by Bird and Mabee, however this study did not focus on condensations so future studies could be conducted regarding the rise of condensations. An alternative is that some elements may be mislabelled. Some elements may have been misidentified as a particular hypural. This is because not all elements were on each section, causing an inferences to be made regarding what some elements were based on the morphological traits of the element (stated in Appendix D, E, F).

It has previously been described that ossification onset begins between 5.0 and 5.5 mm SL for most elements (excluding hypural 5), and fully formed bone also occurred between 5.0 and 5.5 mm SL (Figure 3). Focusing on the two primarily studied elements, hypural 2 and 3, further support of the timings of ossification is shown (Figure 13). Hypural 2 and 3 had an onset of ossification around 5.0 mm, supporting Bird and Mabee (2003) listed timings, a comparison is shown between the outlined Bird and Mabee timings and what was found during this study in Figure 13. However, fully formed bone was only found on one of the four samples in group 1, where fully formed bone was expected. This could indicate that the specimens measured may have been 5.0 mm SL and 5.1 mm SL, since the size was rounded to 5.0 mm SL and not the exact measurement, when no bone has yet to form. There are several alternative explanations for why this could have occurred, including shrinkage of the specimen during the fixation process and defining ossification slightly differently from Bird and Mabee (2003).

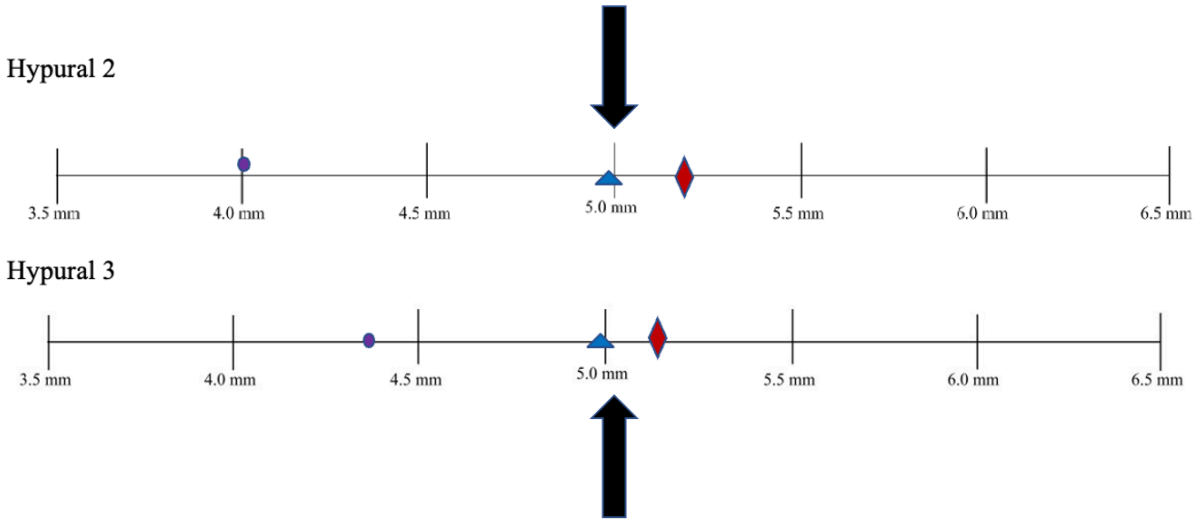

Figure 13. Ossification onset observations shown on timeline of ossification from previous literature of hypurals 2 and 3 (Bird & Mabee, 2003). Purple dots indicate the earliest presence of the condensation from previous literature, blue triangles indicate earliest ossification onset from previous literature, and red diamonds indicate the first presence of fully formed bone from previous literature, black arrows indicate onset of ossification observed within this study.

4.3 Chondrocyte morphology changes

A strange pattern was found between hypural 2 and 3 in regard to the size of their zone of flattened chondrocytes over time. The data indicated that the zone of flattened chondrocytes decreased going to the middle group (5.5 to 7.99 mm SL zebrafish), but increased in the final group studied (8.0 to 9.5 mm SL). There are several potential explanations that could explain the pattern, including the cell death of the hypertrophic chondrocytes.

Regulated cell death of hypertrophic chondrocytes is required for ossification to proceed, as it is required for the bone cells (osteoblasts, osteoclasts, and osteocytes) to be able to invade the cartilaginous matrix (Mackie et al., 2008). Regulated cell death occurs after the chondrocytes have undergone hypertrophy (Franz-Odendaal et al., 2006). The exact mode of cell death is argued between apoptosis and autophagic cell death, with apoptosis causing the cells to flatten

while changes to the morphology made by autophagic cell death have not been well studied (Mackie et al., 2008; Schwartz, 2021). Using histology to look at the morphological changes to the hypertrophic cells may be able to provide more insight into the mode and location of cell death within larval zebrafish caudal fins. Using histology beyond 9 mm SL may also provide support for the idea that the chondrocyte morphology changes is due to cell death, as one could investigate what further changes are made as ossification proceeds. The re-occurrence of the zone of flattened chondrocytes due to regulated cell death would be supported if the histology shows that the zone of flattened chondrocytes differentiates into bone soon after. This would indicate that osteoblasts have embedded into the matrix meaning that the re-occurrence was due to cell death causing the cells to become flattened.

Another potential explanation for the increase of flattened chondrocytes in the larval zebrafish tail is that there may be delayed hypertrophy. Meaning hypertrophy is occurring later than expected within the samples of group 3. There are some mammals that have displayed diseases in which hypertrophy can get delayed (Peck et al., 2015). This is due to improper regulation of *Sox9*, a transcription factor that causes mesenchymal cells to differentiate into cartilage (Carlson, 2019; Peck et al., 2015). The delay in hypertrophy seen in group 3 may be due to an issue with the *Sox9* protein. Previous research has shown that *Sox9* misexpression can impact the process of ossification (Eames et al., 2004). In order to determine whether misexpression of *Sox9* could have resulted in delayed ossification in the larval zebrafish, RNA in situ hybridization should be used to look at the expression of *Sox9*, alongside histology to investigate any further morphological changes to the chondrocytes.

Only 27% of the chondrocytes in the hypurals and parhypural have undergone hypertrophy. This indicates that some unknown factors are potentially constraining the size of

the hypertrophic zone, not allowing it to proceed beyond to the entire element. Previous studies have been found that external factors such as gravity and vibrations can impact bone and bone development within zebrafish (e.g. Aceto et al., 2015; Jeradi & Franz-Odendaal, 2022) Jeradi and Franz-Odendaal (2022) found that vibrations to samples starting from 4 dpf can result in the discontinuation of hypurals and the parhypural, noticeable during the study range (5.5 to 6.5mm SL) investigated throughout this research. These external factors may be impacting the expression of *Sox9*, which could explain why the chondrocyte morphological changes that were observed are not what were expected (Jeradi & Franz-Odendaal, 2022).

4.4 Histological issues

The measurements of histological sections have issues due to the angle of the fin when it was embedded. Any variation within the angle that the tail is positioned at during embedding can provide a different amount of the hypural or parhypural that is investigated. Only ~33% (3/9) of the zebrafish had their hypurals and parhypural flat (attached to both the base and the fin rays). To fix this issue in future research constant adjustments to the sample during the embedding stage may help to ensure that the sample is not angled. Pre-embedding using an agarose mold has previously been found to fix orientation issues (Copper et al., 2018). Specifically using a "shoe mold" while pre-embedding the sample in agarose will limit any bending that may occur to the caudal fin region, mitigating any potential changes in angles that could result in an angle of cut that causes the hypurals and parhypural to not be flat.

4.5 Future research

In order to understand more about the ossification of the five hypurals and the parhypural within zebrafish, more research on ossification on samples 9.0 mm SL and above should be conducted. Looking beyond 9.0 mm SL will allow future researchers to determine the type of ossification that occurs. Within my study perichondral ossification was indicated by the outer

edges being the only region to have fully formed bone. However, there is still the possibility that endochondral ossification is the mode of ossification. This could be tested by investigating if the ossification proceeds medially, replacing the cartilaginous inner parts of the six elements with bone. Looking at zebrafish beyond 9.0 mm SL would also provide more insight into the pattern of chondrocyte hypertrophy.

One limitation to my study was the small sample size. Future replications may provide more insight into the histology of ossification within larval zebrafish. A larger sample size may be able to further support the patterns of growth, or may be able to show that my data was heavily impacted by individual variation. One issue with my data was that it was not normal. A larger sample size may see normal distribution and allow for other statistical tests that can provide more insight into the changes occurring within the zebrafish

4.6 Zebrafish ossification compared to other species

Comparing ossification of the six elements studied to other bones in other model organisms continues to see similar patterns. One such pattern is the direction of growth. When comparing larval zebrafish bone growth to limb growth in mice, both display a proximal to distal growth pattern, with ossification proceeding in the proximal tips before the distal tips (Patton & Kaufman, 1995). Another interesting comparison between larval zebrafish tail ossification and mouse limb ossification is that there is a delay in ossification. It has been found that ossification within the metacarpals were delayed, well after ossification was expected to occur in mice (Patton & Kaufman, 1995). In the zebrafish studied for this research, there was a far lower percentage of cells that had undergone hypertrophy than expected. This indicates that this delay in hypertrophy of the chondrocytes may be similar to the delay of ossification found in mice. Both species have a delayed mechanism (hypertrophy or ossification centre formation) that impacts bone development. Chicken limb development also is similar to the development of

larval zebrafish tails. The bone formation follows a bidirectional pattern in chicken limb bones, with the medial part of the bones forming first (Holder, 1978). This is similar to the formation of the bone edges found on the hypurals and parhypurals of the zebrafish (Appendix E). For both the chicken and the zebrafish ossification will proceed to the proximal tips first before continuing to the distal tip. The chicken will finish ossification after hatching, while the zebrafish will finish ossifying around 24 mm SL(Bird & Mabee, 2003; Holder, 1978). Limb development is embryonic for both chicken and mice, unlike the zebrafish (Bird & Mabee, 2003; Holder, 1978, Patton & Kaufman, 1995). While both chicken and mouse limb development do share similarities with the ossification of larval zebrafish tails, they differ in the mode of ossification. Both chicken and mice undergo endochondral ossification, while zebrafish have ossification indicative of perichondral ossification (Holder, 1978; Patton & Kaufman, 1995). This separates zebrafish as a model specimen from chicken and mice. Perichondral ossification could be studied using zebrafish as the model species, while chicken and mice could be used for endochondral ossification.

Endochondral ossification in mammals proceeds from the fetus until the organism reaches full skeletal development (Rolian, 2020). This study investigated the initial processes of ossification of the caudal fin of zebrafish, however the hypurals and parhypural are not fully developed until the fish have reached around 24 mm SL (Bird & Mabee, 2003). One of the first stages of endochondral ossification within mammals is a bone collar forming, with the edges of the medial part of the cartilaginous template replaced with bone (Rolian, 2020). The same cellular processes in mammals are found in zebrafish for the initial stages of ossification, with the laying down of a cartilaginous template, and the same morphological changes to the

chondrocytes (Thompson et al., 2015). However, the mode of ossification between the elements studied, and mammalian long bones are not the same.

The similarities between the ossification of mammalian long bones and the zebrafish caudal fin further supports using zebrafish as a model organism to learn more about the skeletal system. Using the zebrafish as a model, more information about skeletal development in humans can be investigated without the use of human subjects. This could further current research into skeletal diseases, recovery from skeletal diseases, and potential cures to human diseases (Thompson et al., 2015; Tonelli et al., 2020).

5 Acknowledgments

I would like to thank Dr Tamara Franz-Odendaal for being my undergraduate thesis supervisor, and mentoring me throughout my research. I would also like to thank Dr Michelle Patriquin for being my reader, and providing me with support while writing my thesis. I would also like to thank Dr Anne Dalziel and Dr Ellie Goud for supporting me throughout the school year and guiding me in how to write a thesis, as well as for helping to learn how to use statistical analysis software. I would like to thank all members of the Franz-Odendaal Bone Development Lab, especially Shea McInnis, Juan-David Carvajal Agudelo, and Tracy Apienti for collecting all fish samples, teaching me all of the techniques and protocols I used throughout my research, and for providing lots of help in the lab. I would also like to thank the Saint Mary's Honours Biology class of 2023 for all of their advice throughout my thesis, and for the moral support they have provided. Finally I would like to thank all of the friends and family who have listened to me talk about bones throughout this past year and for all of the support they have provided me in the past, and the future.

References

Aceto, J., Nourizadeh-Lillabadi, R., Marée, R., Dardenne, N., Jeanray, N., Wehenkel, L., Aleström, P., Loon, J. J. W. A. van, & Muller, M. (2015). Zebrafish Bone and General Physiology Are Differently Affected by Hormones or Changes in Gravity. *PLOS ONE*, *10*(6), e0126928. https://doi.org/10.1371/journal.pone.0126928

Bensimon-Brito, A., Cancela, M. L., Huysseune, A., & Witten, P. E. (2012). Vestiges, rudiments and fusion events: The zebrafish caudal fin endoskeleton in an evo-devo perspective. *Evolution & Development*, *14*(1), 116–127. https://doi.org/10.1111/j.1525-142X.2011.00526.x

Bergen, D. J. M., Kague, E., & Hammond, C. L. (2019). Zebrafish as an Emerging Model for Osteoporosis: A Primary Testing Platform for Screening New Osteo-Active Compounds. *Frontiers in Endocrinology*, *10*. https://www.frontiersin.org/articles/10.3389/fendo.2019.00006

Bird, N. C., & Mabee, P. M. (2003). Developmental morphology of the axial skeleton of the zebrafish, Danio rerio (Ostariophysi: Cyprinidae). *Developmental Dynamics: An Official Publication of the American Association of Anatomists*, *228*(3), 337–357. https://doi.org/10.1002/dvdy.10387

Blumer, M. J. F. (2021). Bone tissue and histological and molecular events during development of the long bones. *Annals of Anatomy - Anatomischer Anzeiger*, *235*, 151704. https://doi.org/10.1016/j.aanat.2021.151704

Boskey, A. L. (2013). Bone composition: Relationship to bone fragility and antiosteoporotic drug effects. *BoneKEy Reports*, *2*, 447. https://doi.org/10.1038/bonekey.2013.181

Briggs, J. P. (2002). The zebrafish: A new model organism for integrative physiology. *American Journal of Physiology-Regulatory, Integrative and Comparative Physiology*, *282*(1), R3–R9. https://doi.org/10.1152/ajpregu.00589.2001

Busse, B., Galloway, J. L., Gray, R. S., Harris, M. P., & Kwon, R. Y. (2020). Zebrafish: An Emerging Model for Orthopedic Research. *Journal of Orthopaedic Research*, *38*(5), 925–936. https://doi.org/10.1002/jor.24539

Carlson, B. M. (2019). Chapter 4—The Skeleton. In B. M. Carlson (Ed.), *The Human Body* (pp. 87–110). Academic Press. https://doi.org/10.1016/B978-0-12-804254-0.00004-1

Cervantes-Diaz, F., Contreras, P., & Marcellini, S. (2017). Evolutionary origin of endochondral ossification: The transdifferentiation hypothesis. *Development Genes and Evolution*, *227*(2), 121–127. https://doi.org/10.1007/s00427-016-0567-y

Copper, J. E., Budgeon, L. R., Foutz, C. A., van Rossum, D. B., Vanselow, D. J., Hubley, M. J., Clark, D. P., Mandrell, D. T., & Cheng, K. C. (2018). Comparative analysis of fixation and embedding techniques for optimized histological preparation of zebrafish. *Comparative Biochemistry and Physiology Part C: Toxicology & Pharmacology*, *208*, 38–46. https://doi.org/10.1016/j.cbpc.2017.11.003

Dietrich, K., Fiedler, I. A., Kurzyukova, A., López-Delgado, A. C., McGowan, L. M., Geurtzen, K., Hammond, C. L., Busse, B., & Knopf, F. (2021). Skeletal Biology and Disease Modeling in Zebrafish. *Journal of Bone and Mineral Research*, *36*(3), 436–458. https://doi.org/10.1002/jbmr.4256

Ding, D.-C., Shyu, W.-C., & Lin, S.-Z. (2011). Mesenchymal Stem Cells. *Cell Transplantation*, *20*(1), 5–14. https://doi.org/10.3727/096368910X

Eames, B. F., Sharpe, P. T., & Helms, J. A. (2004). Hierarchy revealed in the specification of three skeletal fates by Sox9 and Runx2. *Developmental Biology*, *274*(1), 188–200. https://doi.org/10.1016/j.ydbio.2004.07.006

Felber, K., Peter Croucher, & Henry H. Roehl. (2010). *Hedgehog signalling is required for perichondral osteoblast differentiation in zebrafish | Elsevier Enhanced Reader*. https://doi.org/10.1016/j.mod.2010.11.006

Franz-Odendaal, T. A., Hall, B. K., & Witten, P. E. (2006). Buried alive: How osteoblasts become osteocytes. *Developmental Dynamics*, *235*(1), 176–190. https://doi.org/10.1002/dvdy.20603

Gemberling, M., Bailey, T. J., Hyde, D. R., & Poss, K. D. (2013). The zebrafish as a model for complex tissue regeneration. *Trends in Genetics*, *29*(11), 611–620. https://doi.org/10.1016/j.tig.2013.07.003

Grandel, H., & Schulte-Merker, S. (1998). The development of the paired fins in the Zebrafish (Danio rerio). *Mechanisms of Development*, *79*(1), 99–120. https://doi.org/10.1016/S0925-4773(98)00176-2

Hall, B. K. (1986). *The role of movement and tissue interactions in the development and growth of bone and secondary cartilage in the clavicle of the embryonic chick*. *93*, 133–152.

Heubel, B. P., Bredesen, C. A., Schilling, T. F., & Le Pabic, P. (2021). Endochondral growth zone pattern and activity in the zebrafish pharyngeal skeleton. *Developmental Dynamics : An Official Publication of the American Association of Anatomists*, *250*(1), 74–87. https://doi.org/10.1002/dvdy.241

Holder, N. (1978). The onset of osteogenesis in the developing chick limb. *Development*, *44*(1), 15–29. https://doi.org/10.1242/dev.44.1.15

Jeradi, S., & Franz-Odendaal, T. A. (2022). Vibration exposure uncovers a critical early developmental window for zebrafish caudal fin development. *Development Genes and Evolution*, *232*(2), 67–79. https://doi.org/10.1007/s00427-022-00691-6

Knowles, H. J., Moskovsky, L., Thompson, M. S., Grunhen, J., Cheng, X., Kashima, T. G., & Athanasou, N. A. (2012). Chondroclasts are mature osteoclasts which are capable of cartilage matrix resorption. *Virchows Archiv*, *461*(2), 205–210. https://doi.org/10.1007/s00428-012-1274-3

Kobayashi-Sun, J., Yamamori, S., Kondo, M., Kuroda, J., Ikegame, M., Suzuki, N., Kitamura, K., Hattori, A., Yamaguchi, M., & Kobayashi, I. (2020). Uptake of osteoblast-derived extracellular vesicles promtoes the differentiation of osteoclasts in the zebrafish scale. *Communications Biology*, *3*. https://doi.org/10.1038/s42003-020-0925-1

Komsta, L. (2022). *Outliers: Tests for Outliers. R package version 0.15*. https://CRAN.R-project.org/package=outliers

Mackie, E. J., Ahmed, Y. A., Tatarczuch, L., Chen, K.-S., & Mirams, M. (2008). Endochondral ossification: How cartilage is converted into bone in the developing skeleton. *The International Journal of Biochemistry & Cell Biology*, *40*(1), 46–62. https://doi.org/10.1016/j.biocel.2007.06.009

Mione, M. C., & Trede, N. S. (2010). The zebrafish as a model for cancer. *Disease Models & Mechanisms*, *3*(9–10), 517–523. https://doi.org/10.1242/dmm.004747

Odgren, P. R., Witwicka, H., & Reyes-Gutierrez, P. (2016). The cast of clasts: Catabolism and vascular invasion during bone growth, repair and disease by osteoclasts, chondroclasts, and septoclasts. *Connective Tissue Research*, *57*(3), 161–174.

Parichy, D. M., Elizondo, M. R., Mills, M. G., Gordon, T. N., & Engeszer, R. E. (2009). Normal table of postembryonic zebrafish development: Staging by externally visible anatomy of the living fish. *Developmental Dynamics*, *238*(12), 2975–3015. https://doi.org/10.1002/dvdy.22113

Patton, J. T., & Kaufman, M. H. (1995). The timing of ossification of the limb bones, and growth rates of various long bones of the fore and hind limbs of the prenatal and early postnatal laboratory mouse. *Journal of Anatomy*, *186*(Pt 1), 175–185.

Peck, S. H., O'Donnell, P. J. M., Kang, J. L., Malhotra, N. R., Dodge, G. R., Pacifici, M., Shore, E. M., Haskins, M. E., & Smith, L. J. (2015). Delayed hypertrophic differentiation of epiphyseal chondrocytes contributes to failed secondary ossification in mucopolysaccharidosis VII dogs. *Molecular Genetics and Metabolism*, *116*(3), 195–203. https://doi.org/10.1016/j.ymgme.2015.09.008

R Core Team. (2022). *R: A language and environment for statistical computing.* [R Foundation for Statistical Computing]. https://www.R-project.org/

Rolian, C. (2020). Endochondral ossification and the evolution of limb proportions. *WIREs Developmental Biology*, *9*(4), e373. https://doi.org/10.1002/wdev.373

Rolland-Lagan, A.-G., Paquette, M., Tweedle, V., & Akimenko, M.-A. (2012). Morphogen-based simulation model of ray growth and joint patterning during fin development and regeneration. *Development (Cambridge, England)*, *139*, 1188–1197. https://doi.org/10.1242/dev.073452

Schwartz, L. M. (2021). Autophagic Cell Death During Development – Ancient and Mysterious. *Frontiers in Cell and Developmental Biology*, *9*. https://www.frontiersin.org/articles/10.3389/fcell.2021.656370

Stockwell, R. A. (1978). Chondrocytes. *Journal of Clinical Pathology*, *31*(Suppl 12), 7–13. https://doi.org/10.1136/jcp.31.Suppl_12.7

Thompson, E. M., Matsiko, A., Farrell, E., Kelly, D. J., & O'Brien, F. J. (2015). Recapitulating endochondral ossification: A promising route to in vivo bone regeneration. *Journal of Tissue Engineering and Regenerative Medicine*, *9*(8), 889–902. https://doi.org/10.1002/term.1918

Tonelli, F., Bek, J. W., Besio, R., De Clercq, A., Leoni, L., Salmon, P., Coucke, P. J., Willaert, A., & Forlino, A. (2020). Zebrafish: A Resourceful Vertebrate Model to Investigate Skeletal Disorders. *Frontiers in Endocrinology*, *11*. https://www.frontiersin.org/articles/10.3389/fendo.2020.00489

Weigele, J., & Franz-Odendaal, T. A. (2016). Functional bone histology of zebrafish reveals two types of endochondral ossification, different types of osteoblast clusters and a new bone type. *Journal of Anatomy*, *229*(1), 92–103. https://doi.org/10.1111/joa.12480

Appendices

Appendix A. Staining protocols

Hydration

1. Citrosolve -> 5 minutes (x2)
2. 100% EtOH -> 1 minute (x2)
3. 90% EtOH -> 1 minute
4. 70% EtOH -> 1 minute
5. 50% EtOH -> 1 minute

HBQ Stain

1. Celestine blue: 5 minutes
2. Wash in H_2O: 1 minute
3. Mayer's Haematoxylin: 5 minutes
4. Wash in H_2O: 1 minute
5. Alcian blue: 5 minute
6. Wash in H_2O: 2 minutes
7. Phosphomolybdic Acid: 1 minute
8. Wash in H_2O: 1 minute
9. Direct red: 5 minutes
10. Rinse inn H_2O: 20 seconds
11. 100% EtOH: 20 seconds
12. 100% EtOH: 20 seconds

Masson's Trichrome Stain

1. Haematoxylin: 10 minutes
2. Rinse: dip in H_2O
3. Scott's Tap Water: 30 seconds
4. Rinse: dip in H_2O
5. Xylidine Ponceau: 2 minutes
6. Rinse: dip in H_2O
7. Phosphomolybdic Acid: 4 minutes
8. Rinse: dip in H_2O
9. Light green: 90 seconds
10. Rinse: dip in H_2O
11. Dip in 100% EtOH
12. Dip in 100% EtOH

Clearing

1. Citrosolve: 1 minute (x4)
2. Dab off excess citrosolve with a kimwipe
3. Coverslip with DPX

Appendix B. Chemical information

Alcian blue 8GX

Brand: Sigma-Aldrich
Product Number: A3157

Celestine blue

Brand: Sigma-Aldrich
Product Number: 206342

Citrosolve

Brand: Fisher Scientific
Product Numbers: 22143975, 22143976, BN08170011

Direct red

Brand: Sigma-Aldrich
Product Number: 195251

DPX mountant

Brand: Sigma-Aldrich
Product Number: 06522

Ethanol

Brand: Greenfield global
Product Number: 64-17-5

Light green

Brand: Sigma-Aldrich
Product Number: L5382-25G

Mayer's Haematoxylin

Brand: Sigma-Aldrich
Product Number: MHS16

Paraplast X-tra Tissue Embedding Medium (paraffin wax)

Brand: McCormick Scientific
Product Number: 39503002

Paraformaldehyde

Brand: Sigma-Aldrich
Product Number: P6148

Phosphomolybdic Acid

Brand: Sigma-Aldrich
Product Number: HT153

Xylidine Ponceau

Brand: Sigma-Aldrich
Product Number: P2395

Appendix C. Recipes

Phosphate Buffered Saline (PBS)

- Dissolve in 800 mL Water:
- 80 g NaCl
- 2 g KCl
- 26.8 g Na_2HPO_4

- Adjust pH to 7.4 with 1M HCl
- Adjust volume to 1L with water

Note: PBS Storage: PBS is stable at room temperature, or can be stored at 4° C

Scott's Tap Water (from Alma)

- 7 g Sodium Bicarbonate
- 40 g Magnesium Sulfate
- 2000 mL water
- (plus thymol)

Add a drop or two, or a tablet of thymol to help preserve the solution if not going through the stock quickly

Appendix D. Group 1 schematics

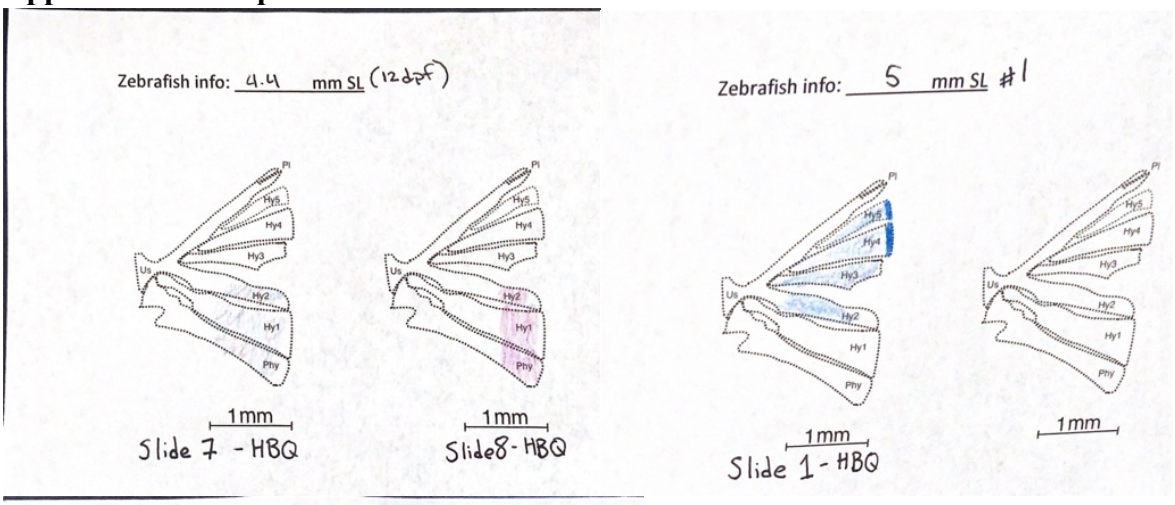

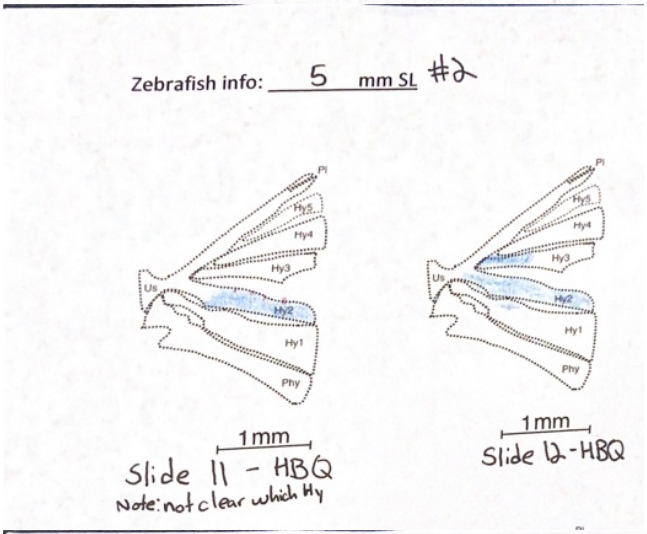

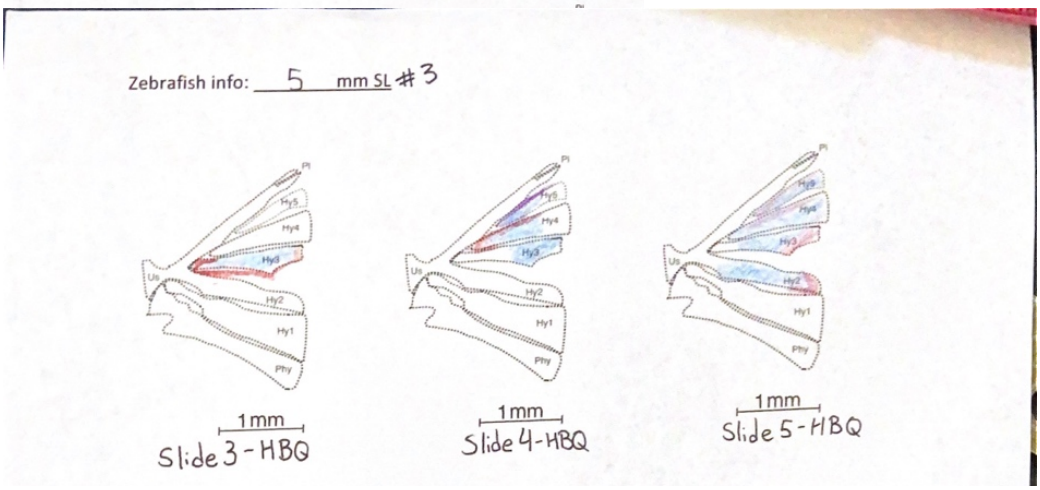

Blue = cartilage, Red = bone, Purple = strange staining

Appendix E. Group 2 schematics

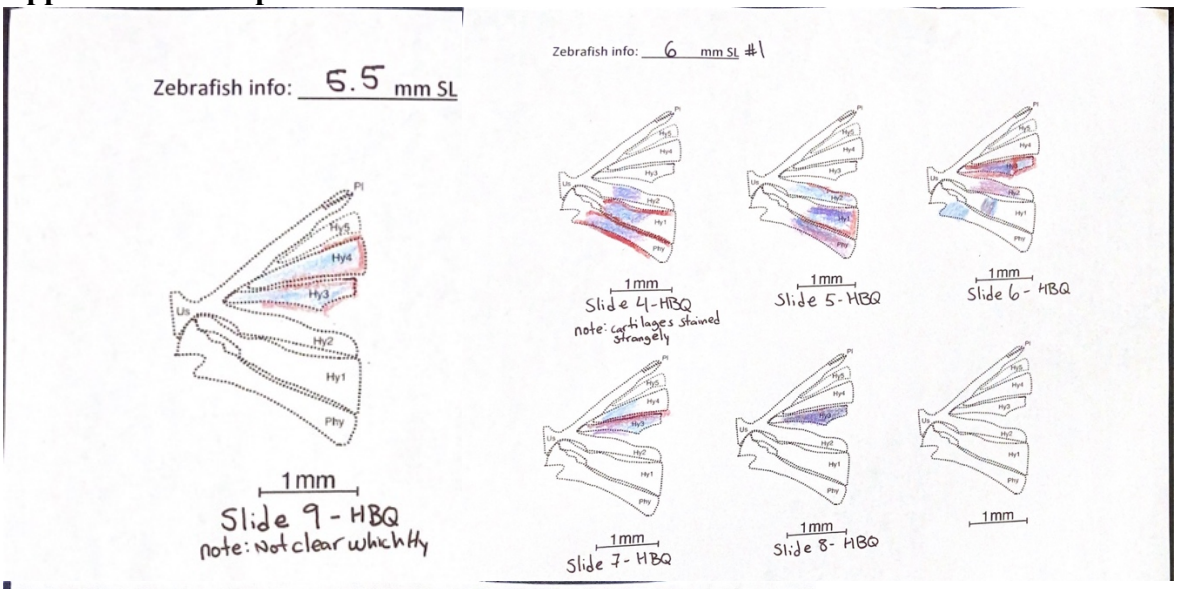

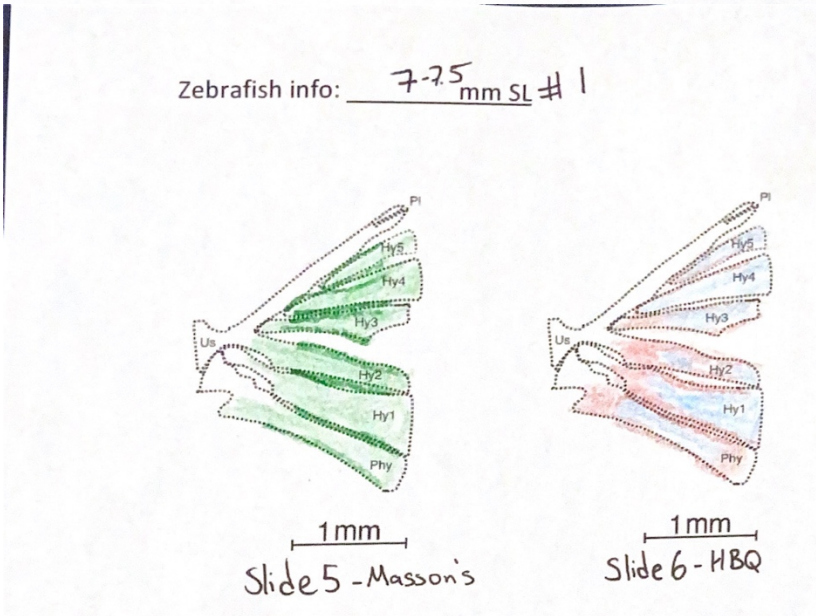

Blue = cartilage, Red = bone, Green = cartilage stained with Masson's Trichrome, Dark Green = bone stained with Masson's Trichrome, Purple = strange staining

Appendix F. Group 3 schematics

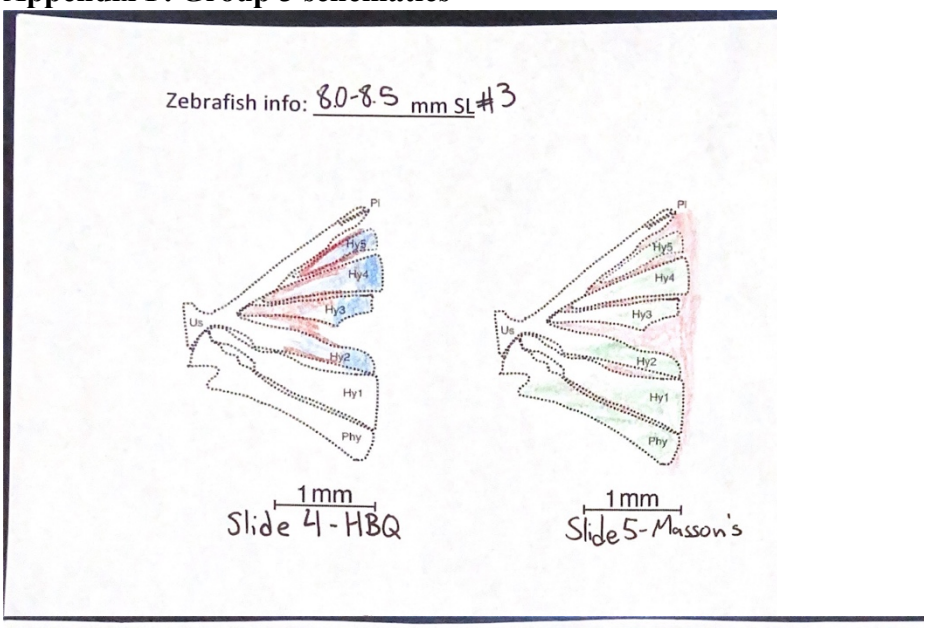

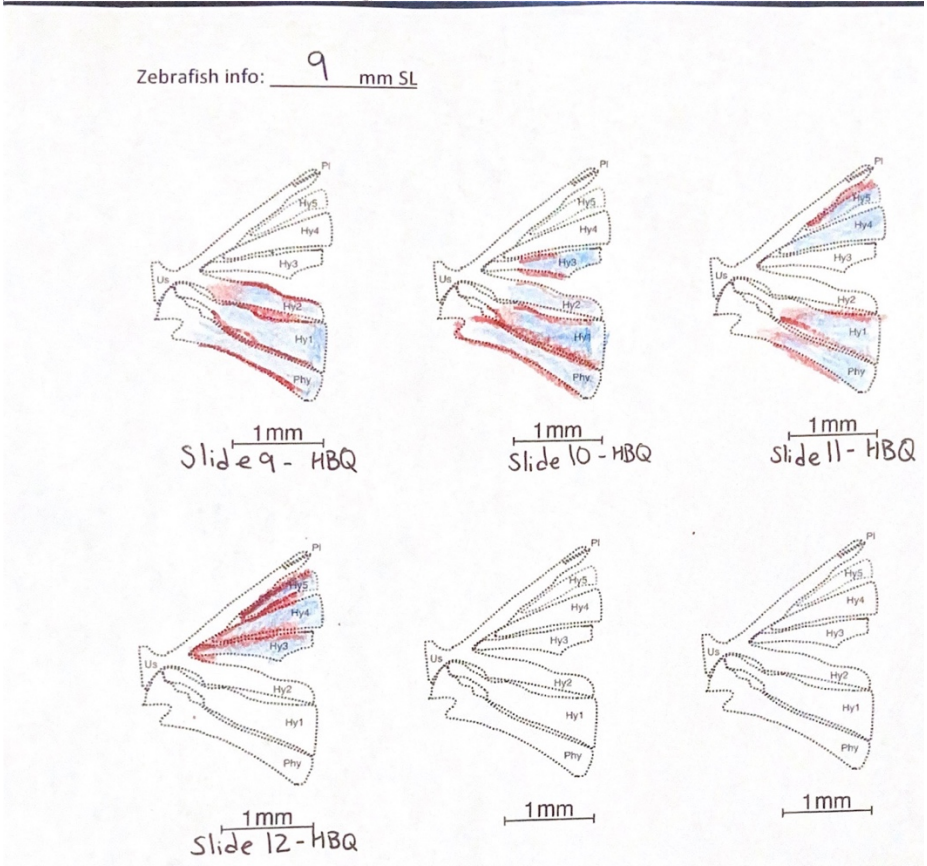

Blue = cartilage, Red = bone, Green = cartilage stained with Masson's Trichrome, Dark Green = bone stained with Masson's Trichrome, Purple = strange staining

Appendix G. Histograms of Total length

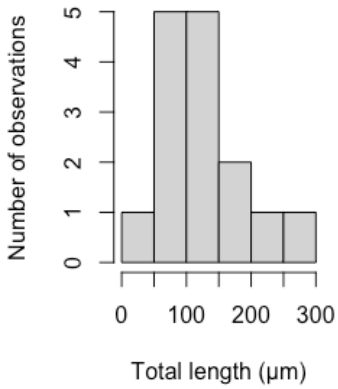

Hypural 2 histogram showing normal distribution of total hypural length (µm)

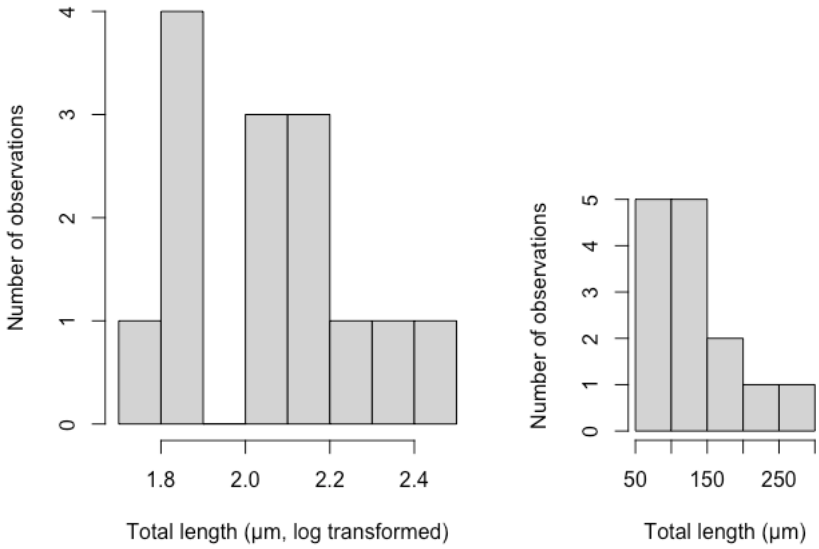

Hypural 3 histogram showing normal distribution of a) log transformed hypural 3 total length (µm), and b) non-log transformed data.

Appendix H. Raw data for all measurements included in mean calculations

All measurements that were collected from each specimen for hypurals 2 and 3. The measurements were averaged for each specimen from the data shown.

Size	Total length (TL)	Flattened Chondrocyte length (FC)	(FC/TL) * 100	Bone element	Group
4.5	45.8	0	0%	hy2	1
5 #1	94.6	38.43	41%	hy2	1
5 #2	134.51	24.27	18%	hy2	1
5 #2	169.83	0	0%	hy2	1
5 #3	69.11	23.84	34%	hy2	1
6	67.03	0	0%	hy2	2
6	153.84	53.94	35%	hy2	2
6	65.15	15.07	23%	hy2	2
7	120.79	0	0%	hy2	2
7	109.46	0	0%	hy2	2
8	57.23	0	0%	hy2	3
8	108.28	24.66	23%	hy2	3
9	246.46	54.35	22%	hy2	3
9	292.53	54.26	19%	hy2	3
9	138.41	51.51	37%	hy2	3
5 #1	164.65	0	0%	hy3	1
5 #3	110.89	27.62	25%	hy3	1
5 #3	69.35	31.09	45%	hy3	1
5 #3	76.36	0	0%	hy3	1
5.5	60.35	6.76	11%	hy3	2
5.5	75.71	0	0%	hy3	2
6	145.4	41.12	28%	hy3	2
6	130.42	57.36	44%	hy3	2
7	155.52	0	0%	hy3	2
7	113.36	0	0%	hy3	2
8	114.36	29.76	26%	hy3	3
8	78.29	25.66	33%	hy3	3
9	246.97	16.55	7%	hy3	3
9	284.27	36.05	13%	hy3	3